The Henryk Niewodniczański
Institute of Nuclear Physics
Polish Academy of Sciences

Understanding physicochemical interactions at the nano-bio interface

Ewa Pięta

Department of Experimental Physics of Complex Systems
Institute of Nuclear Physics
Polish Academy of Sciences
Krakow, Poland

Presentation schedule & research motivation

- *Density Functional Theory (DFT)*
- *Raman Spectroscopy*
- *Infrared Absorption Spectroscopy*

Nanoparticles
- *Synthesis (IKiFP PAN)*
- *UV-Vis*
- *TEM*
- *SEM*

Monitoring the adsorption process:
- *SERS*
- *SEIRA*
- *SEIRA in nanoscale*

- *Introducing NPs inside the cells*
- *Correlative imaging*
- *drug/nanoparticles conjugates*

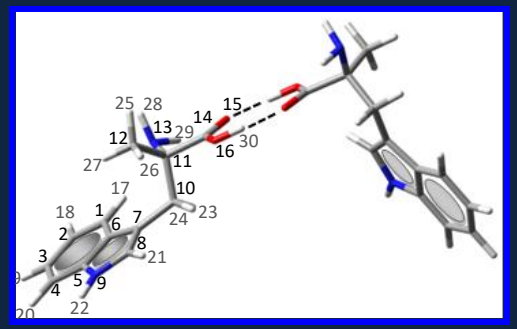

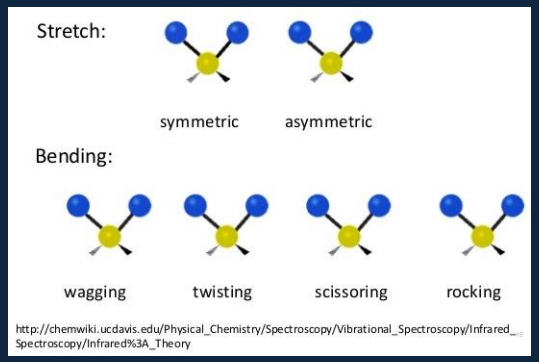

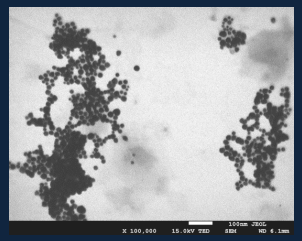

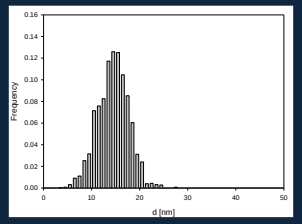

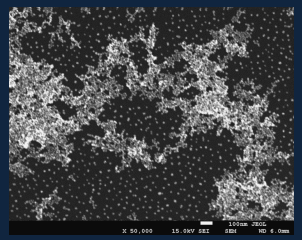

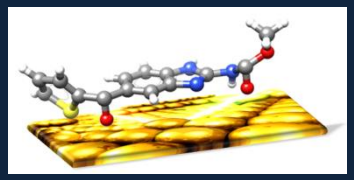

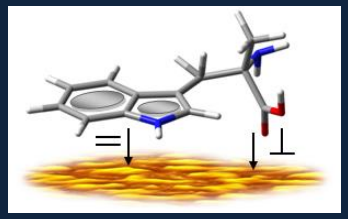

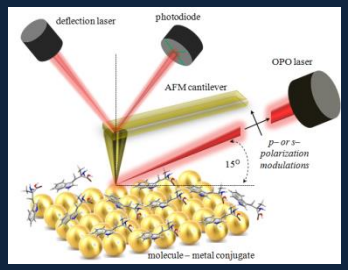

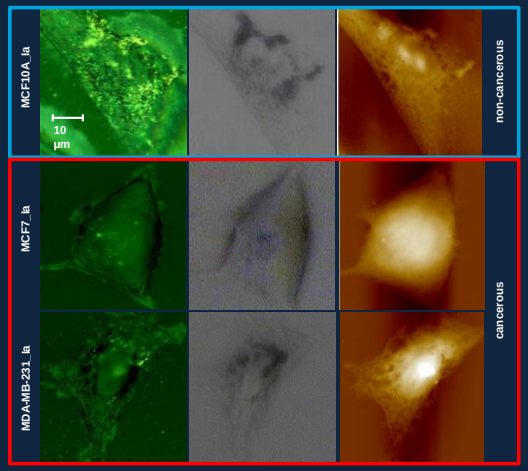

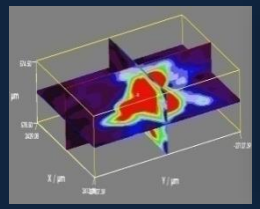

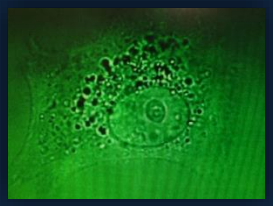

Surface-enhanced techniques in vibrational spectroscopy

- SERS *(Surface Enhanced Raman Spectroscopy)*
  - enhancement factor up to 10^{14}

Volume 26, number 2 CHEMICAL PHYSICS LETTERS 15 May 1974

RAMAN SPECTRA OF PYRIDINE ADSORBED AT A SILVER ELECTRODE

M. FLEISCHMANN, P.J. HENDRA and A.J. McQUILLAN
Department of Chemistry, The University, Southampton SO9 5NH, UK

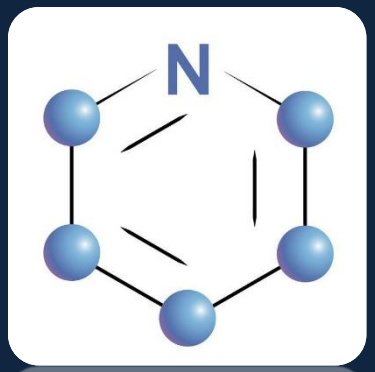

- SEIRA *(Surface Enhanced Infrared Absorption Spectoscopy)*
  - enhancement factor up to 10^{3}

Surface-Enhanced Infrared Spectroscopy: The Origin of the Absorption Enhancement and Band Selection Rule in the Infrared Spectra of Molecules Adsorbed on Fine Metal Particles

MASATOSHI OSAWA,* KEN-ICHI ATAKA, KATSUMASA YOSHII, and YUJI NISHIKAWA
Department of Molecular Chemistry and Engineering, Faculty of Engineering, Tohoku University, Aoba, Aramaki, Aoba-ku, Sendai 980, Japan (M.O., K.A., K.Y.); and Analytical Center, Konica Corporation, No. 1 Sakura-machi, Hino-shi, Tokyo 191, Japan (Y.N.)

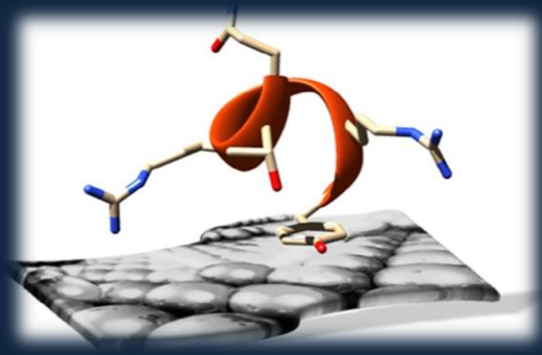

Enhancement mechanisms in vibrational spectroscopy

electromagnetic mechanism

- the studied molecule is adsorbed onto metal surface or is located in close proximity to this substrate
- direct contact of the molecule with the metal surface is not required, but the enhancement decreases significantly with the increase of this distance, determined by the disappearance of the dipole field of metal at a distance [1/d][12]
- enhancement is particularly strong in the "hot spots", in SERS up to 10^{15}.

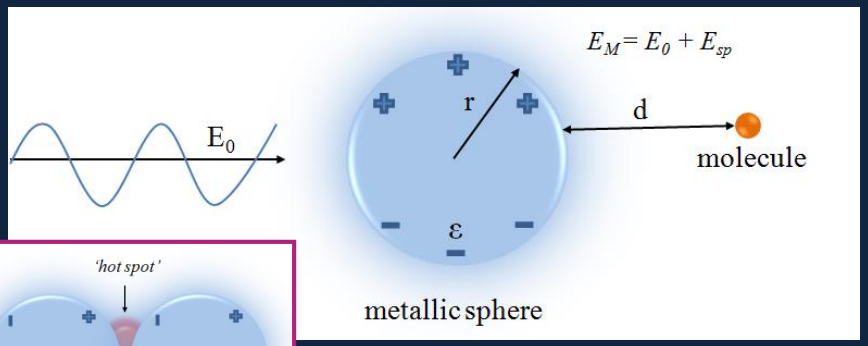

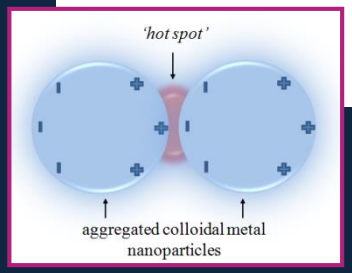

chemical mechanism

- the studied molecule is chemically binds to the metal substrate
- it is not well known
- an electron coupling between a compound molecule and a metal and forming an adsorbate-surface complex
- *charge-transfer* in SERS
- Up to 10^2 contribution theoretically

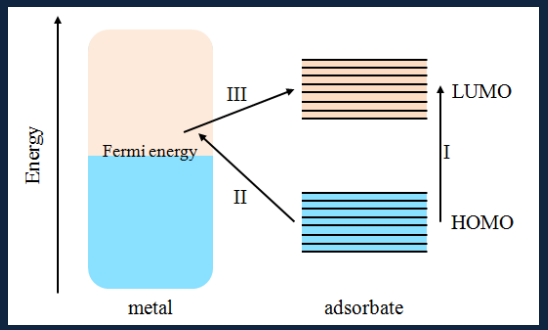

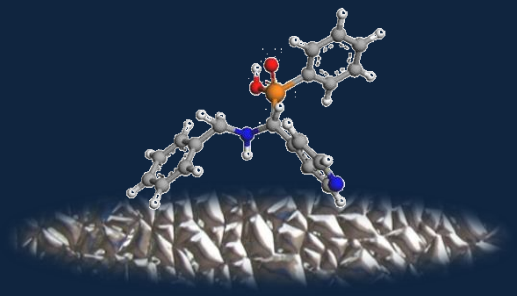

E. Smith, G. Dent, Modern Raman spectroscopy. A practical approach, John Wiley & Sons, Ltd: Chichester, 2005, 71−133
K.A. Willets, Chem. Soc. Rev. 2014, 43, 3854
R.C. Maher, SERS Hot Spots, w: Raman Spectroscopy for Nanomaterials Characterization, red. C.S.S.R. Kumar, 2012, 215–260
M. Osawa, Surface-enhanced infrared absorption, in: S. Kawata (Ed.), Near-Field Optics and Surface Plasmon Polaritons, Topics in Applied Physics, 81 (2001), Springer, Heidelberg, Germany, 163-187.

Surface selection rules

Surface selection rules

J. Chem. Phys., Vol. 77, No. 9, 1 November 1982

M. Moskovits

Department of Chemistry and Erindale College, University of Toronto, Toronto M5S 1A1, Canada

(Received 20 April 1982; accepted 23 July 1982)

Surface Science 124 (1983) 209–219 209
North-Holland Publishing Company

SURFACE RAMAN ELECTROMAGNETIC ENHANCEMENT FACTORS FOR MOLECULES AT THE SURFACE OF SMALL ISOLATED METAL SPHERES: THE DETERMINATION OF ADSORBATE ORIENTATION FROM SERS RELATIVE INTENSITIES

J.A. CREIGHTON

Chemical Laboratories, University of Kent, Canterbury CT2 7NH, UK

ACADEMIC PRESS

Available online at www.sciencedirect.com
SCIENCE DIRECT®

Journal of Colloid and Interface Science 263 (2003) 357–363

JOURNAL OF Colloid and Interface Science

www.elsevier.com/locate/jcis

Vibrational study of the metal–adsorbate interaction of phenylacetic acid and α-phenylglycine on silver surfaces

J.L. Castro,* M.R. López Ramírez, I. López Tocón, and J.C. Otero

J. Phys. Chem. C **2008**, *112*, 5605−5617 **5605**

A Unified Approach to Surface-Enhanced Raman Spectroscopy

John R. Lombardi* and Ronald L. Birke

Department of Chemistry, The City College of New York, New York, New York 10031

Three classes of vibrational modes with distinct spectral behavior:

(1) normal component of the field and resulting in an induced dipole with a strong component only in a direction perpendicular to the surface;

(2) tangential component of the field and resulting in an induced dipole with a strong component tangential to the surface;

(3) the mixed cases (for example, a normal field exciting a dipole with a strong component parallel to the surface).

Vibrations characteristic for the aromatic ring are classified into four symmetry groups, i. e. A1, A2, B1, and B2. The ratio of the surface enhancement factors for the A2, B1 and B2 vibrational modes are 4:1:1 for a flat orientation of aromatic molecule, and 1:1:4 for a vertical arrangement.

Significant enhancement of bands due to the A2 group vibrations (out of plane) is connected with flat position of the ring, whereas the vertical orientation is manifested by strong enhancement of spectral signals attributed to the B2 group oscillations (in plane).

No metal-aromatic ring interaction unless there is significant down-shifts in wavenumber of the ring mode bands and clear changes in their widths

Three types of resonance contribute to the SERS enhancement, including surface plasmon resonance, the molecular resonance and the metal-molecule charge-transfer.

SERS&SEIRA – active substrates

nanoparticles

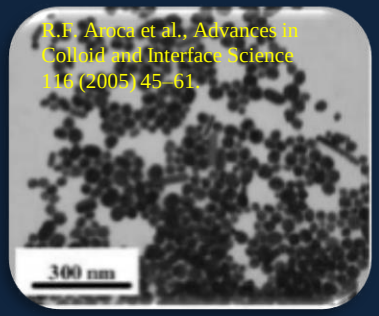

R.F. Aroca et al., Advances in Colloid and Interface Science 116 (2005) 45–61.

nanostars

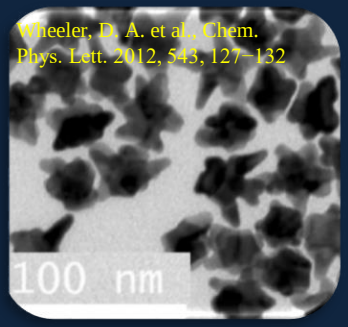

Wheeler, D. A. et al., Chem. Phys. Lett. 2012, 543, 127−132

nanopillars

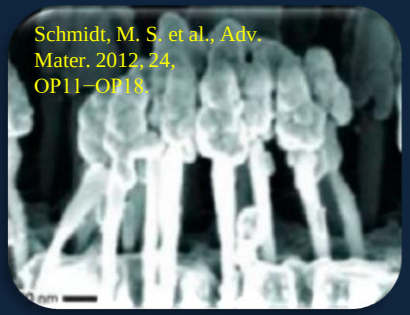

Schmidt, M. S. et al., Adv. Mater. 2012, 24, OP11−OP18.

nanosquares

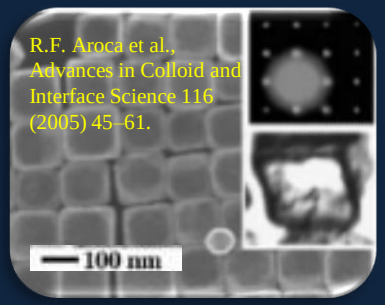

R.F. Aroca et al., Advances in Colloid and Interface Science 116 (2005) 45–61.

electrodes

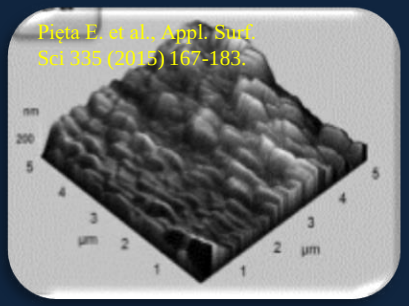

Pięta E. et al., Appl. Surf. Sci 335 (2015) 167-183.

“rational” substrates?

nanorods

Milliken, S. et al., Spectrochim. Acta, Part A 2018, 196, 222−228

nanowires

R.F. Aroca et al., Advances in Colloid and Interface Science 116 (2005) 45–61.

“hedgehog particles”

Montjoy, D. G. et al., J. Am. Chem. Soc. 2018, 140, 7835−7845.

nanoshells

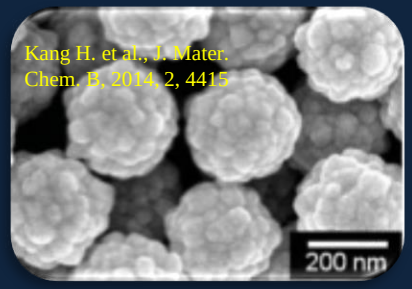

Kang H. et al., J. Mater. Chem. B, 2014, 2, 4415

Applied Surface Science 404 (2017) 168–179

Contents lists available at ScienceDirect

Applied Surface Science

journal homepage: www.elsevier.com/locate/apsusc

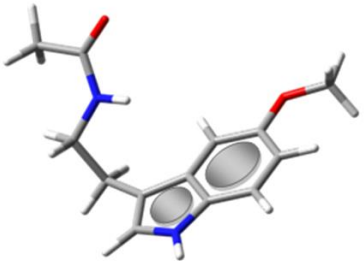

Full Length Article

Potential drug – nanosensor conjugates: Raman, infrared absorption, surface – enhanced Raman, and density functional theory investigations of indolic molecules

Ewa Pięta[a,*], Czesława Paluszkiewicz[a], Magdalena Oćwieja[b], Wojciech M. Kwiatek[a]

[a] Institute of Nuclear Physics, Polish Academy of Sciences, PL-31342 Krakow, Poland
[b] J. Haber Institute of Catalysis and Surface Chemistry, Polish Academy of Sciences, PL-30239 Krakow, Poland

AuNPs

PCCP

PAPER

Check for updates

Cite this: Phys. Chem. Chem. Phys., 2018, 20, 27992

Multianalytical approach for surface- and tip-enhanced infrared spectroscopy study of a molecule–metal conjugate: deducing its adsorption geometry

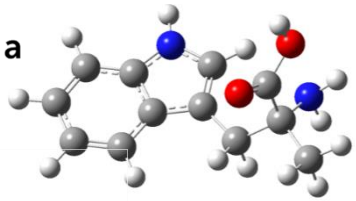

E. Pięta, * C. Paluszkiewicz and W. M. Kwiatek

biocompatibility with DNA, RNA, amino acids and proteins

precise control of distribution and metabolism of drugs in cells

the appropriate NPs diameter

defining the sensitivity of cells to drugs

THE JOURNAL OF PHYSICAL CHEMISTRY C

Article

pubs.acs.org/JPCC

Monitoring the Interfacial Behavior of Selective Y5 Receptor Antagonist on Colloidal Gold Nanoparticle Surfaces: Surface-Enhanced Vibrational Spectroscopy Studies

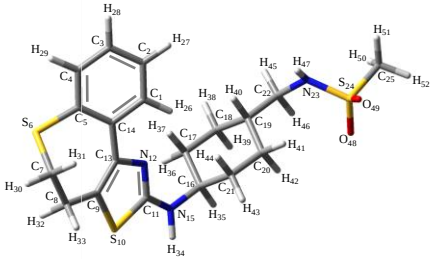

Ewa Pięta,*,† Natalia Piergies,† Magdalena Oćwieja,‡ Helena Domin,§ Czesława Paluszkiewicz,† Elżbieta Bielańska,‡ and Wojciech M. Kwiatek†

†Institute of Nuclear Physics Polish Academy of Sciences, PL-31342 Krakow, Poland
‡J. Haber Institute of Catalysis and Surface Chemistry Polish Academy of Sciences, PL-30239 Krakow, Poland
§Institute of Pharmacology, Polish Academy of Sciences, Department of Neurobiology, 31-343 Krakow, Smetna Street 12, Poland

S. Muthuirulappan et al. *Asian Pac. J. Cancer Prev.* 14 (2013) 2213.
A.G. Najar et al., *Asian Pac. J. Cancer Prev.* 14 (2013) 495.
J. Lee et al. *Cancer Lett.* 347 (2014) 46.
O.C. Farokhzad et al. *ACS Nano* 3 (2009) 16.

In the search of effective nanosensors

AuNPs synthesis & UV-Vis spectra

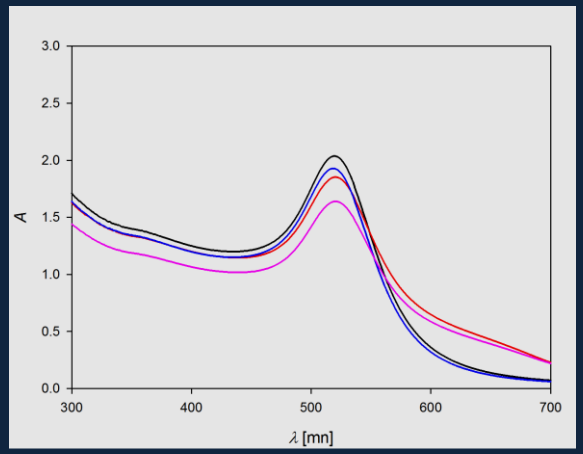

Legend:

(—) the pure suspensions of concentration equal to 60 mg L^{-1}
(—) the suspension of ionic strength 0.03 mol dm^3 NaCl
(—) the suspensions with the drug of concentration 10^{-4} mol dm^3
(—) the suspension of ionic strength 0.03 mol dm^3 and the drug.

TEM image of AuNPs & particle size distribution

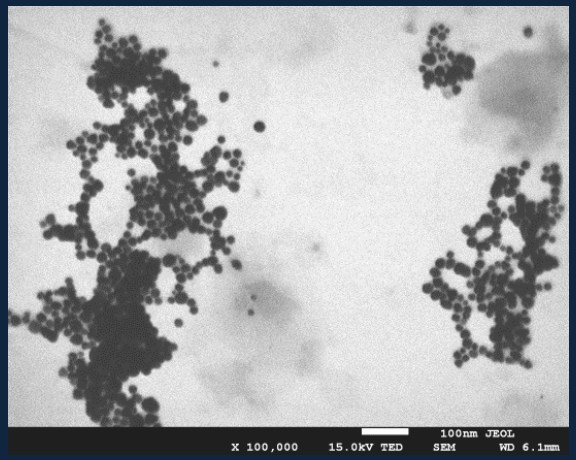

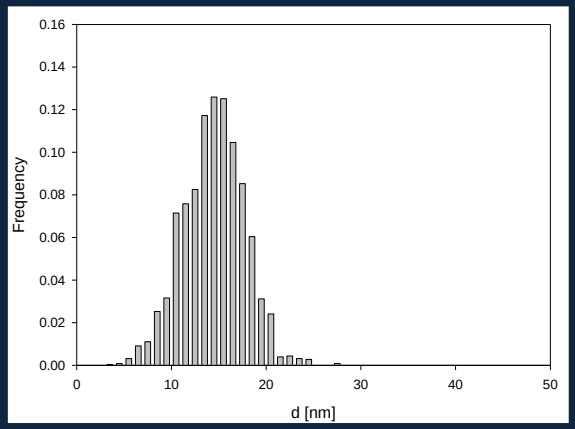

SEM images of AuNPs & AuNPs/drug conjugate

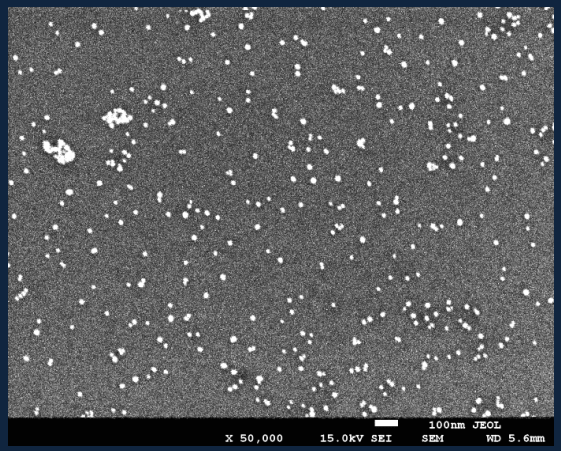

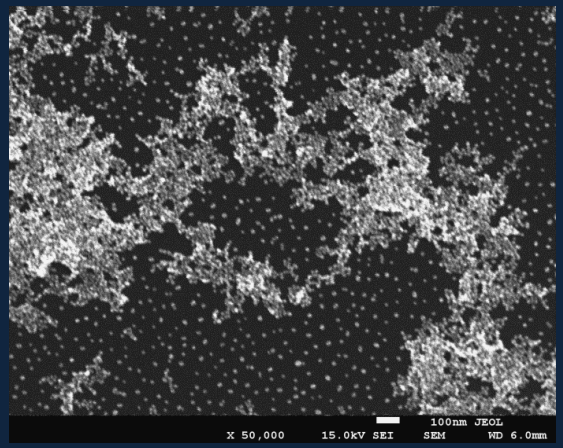

E. Pięta, C. Paluszkiewicz, M. Oćwieja, W. M. Kwiatek, *Applied Surface Science* 404 , **2017**, 168-179.
E. Pięta, N. Piergies, M. Oćwieja, H. Domin, C. Paluszkiewicz, E. Bielańska, W. M. Kwiatek, *J. Phys. Chem. C* 121, **2017**, 17276−17288.

α-methyl-DL-tryptophan
Molecular structure, DFT calculations

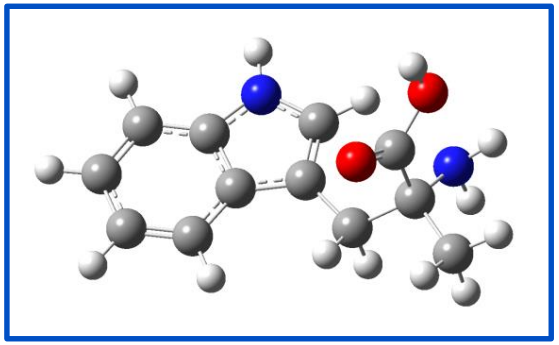

- synthetic amino acid, tryptophan analogue and serotonin precursor
- potential antitumor activity
- indole ring, tetrahedral carbon atom
- cyclic dimer formed by a pair of intermolecular hydrogen bonds between the hydrogen atom of the carboxyl group and the oxygen atom of this group from the second monomer

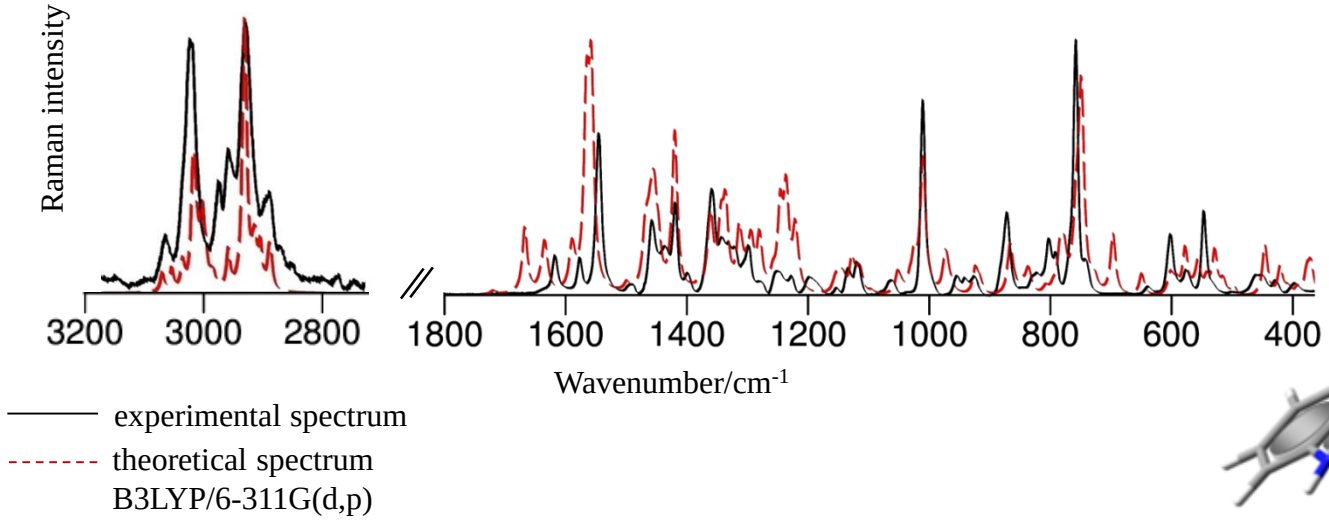

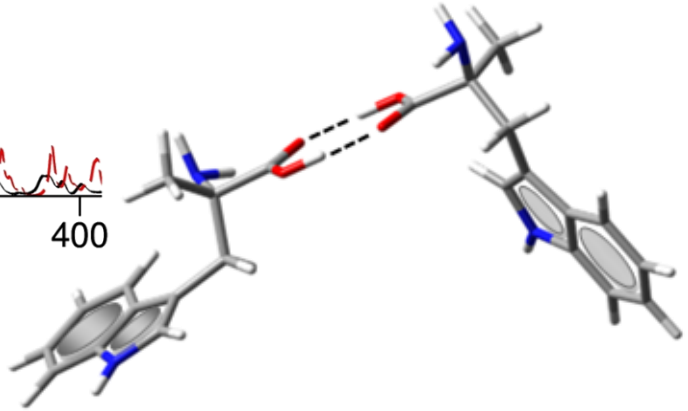

α-methyl-DL-tryptophan RS vibrations

InVia Renishaw Spectrometer integrated with atomic force microscope

Ind ring

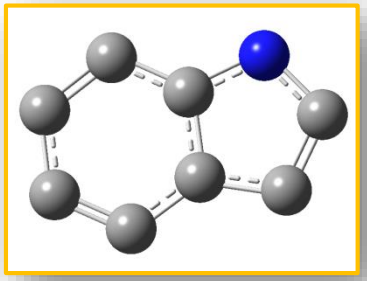

amino group

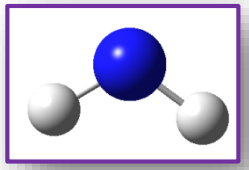

methylene group

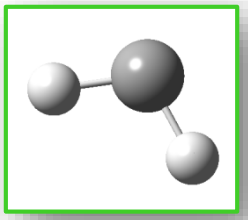

- exc. wavelength: 785 nm
- CCD detector
- 100× magn. objective
- spectral resolution 1 cm^{-1}
- laser power 100 mW

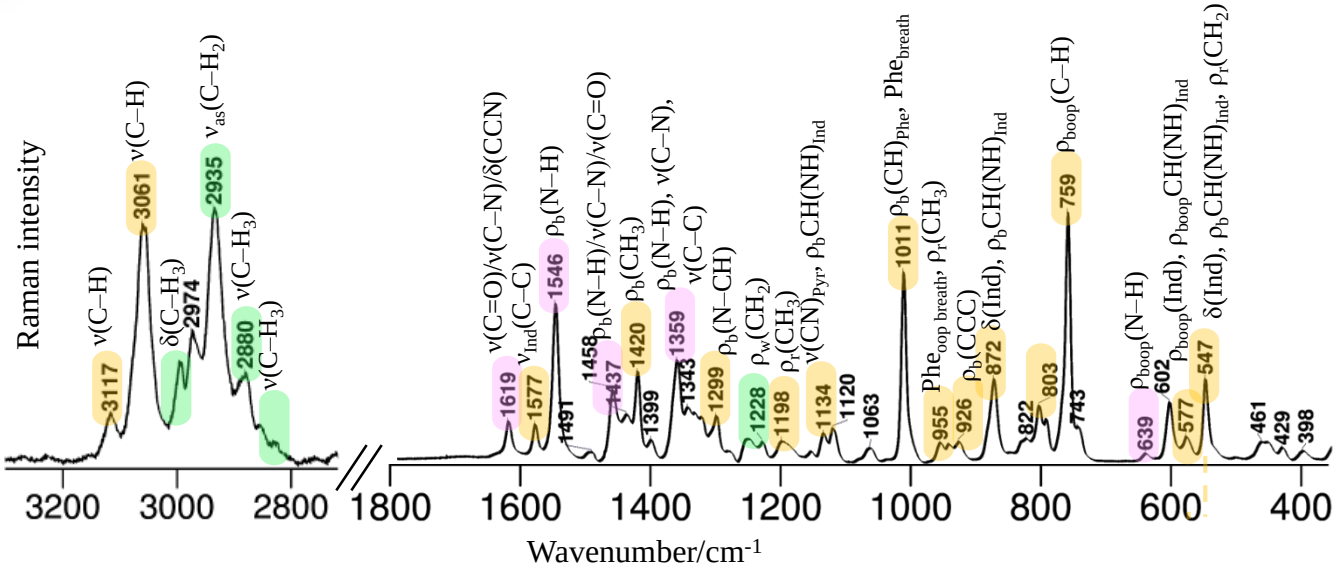

E. Pięta, C. Paluszkiewicz, M. Oćwieja, W. M. Kwiatek, *Applied Surface Science* 404 , **2017**, 168-179.

FTIR & SEIRA
various measurement modes vs. the way of adsorption

Thermo Scientific
Nicolet™ iS™ 5 FT-IR Spectrometer

- ATR/ZnSe
- DTGS detector
- spectral resolution: 4 cm^{-1}
- c ~10^{-4} M

Thermo Scientific™ Nicolet™ iN™10
MX Infrared Imaging Microscope

- transmission
- MCT linear array detector
- spectral resolution: 4 cm^{-1}
- c ~10^{-4} M

- NH z Ind & CO: strong interaction with AuNPs
- CH_2 i CH_3: moved away from the AuNPs surface

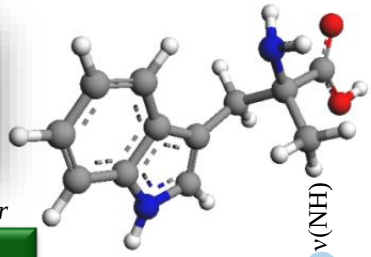

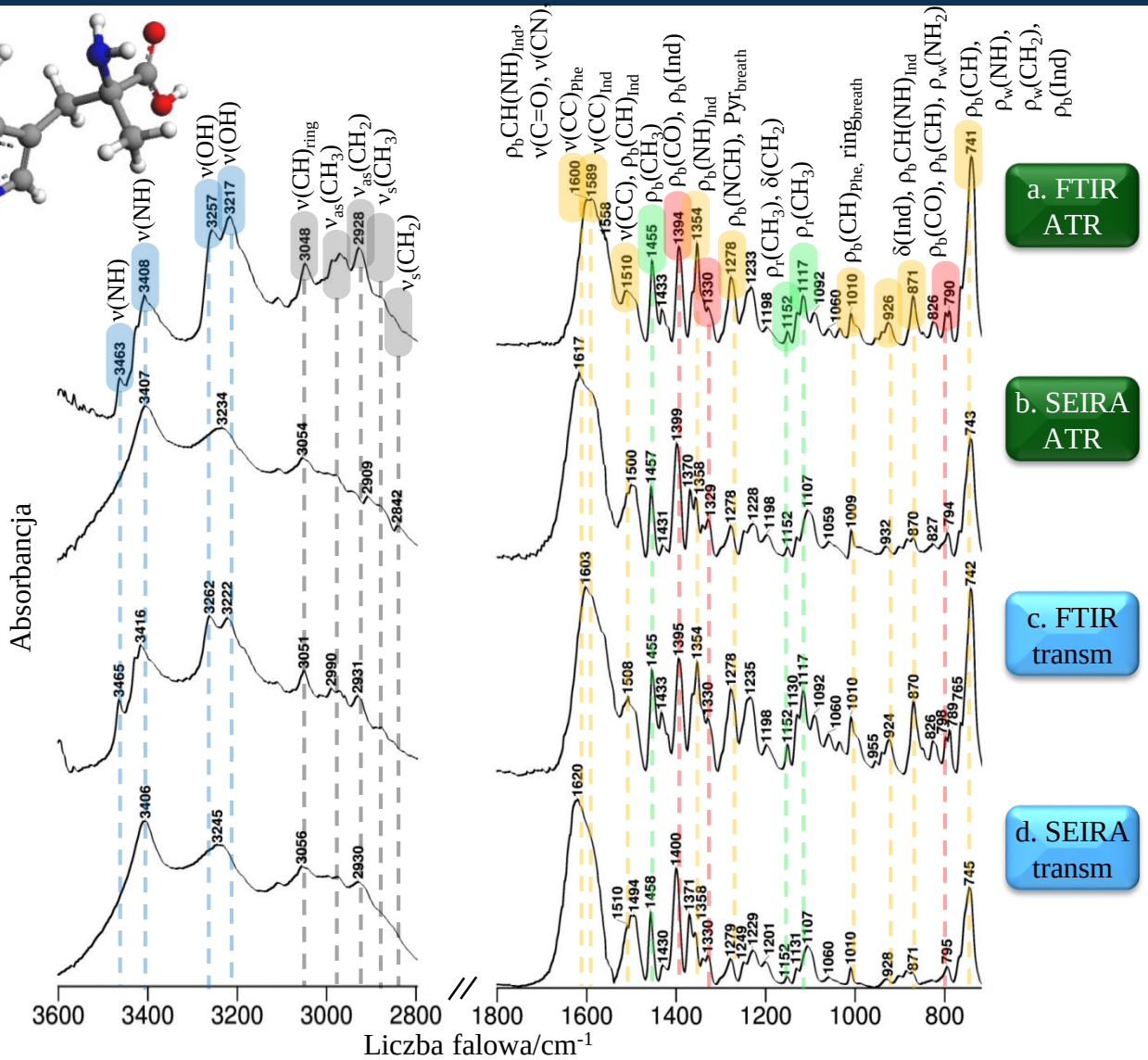

SEIRA
different incident angles & the adsorption geometry prediction

Seagull™ Variable Angle Reflection Accessory

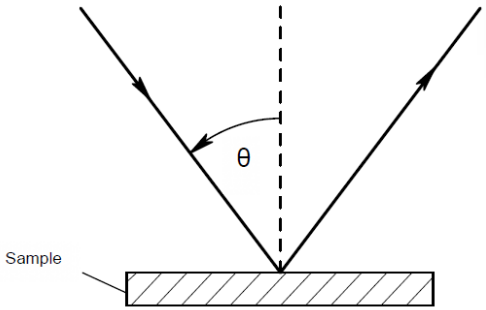

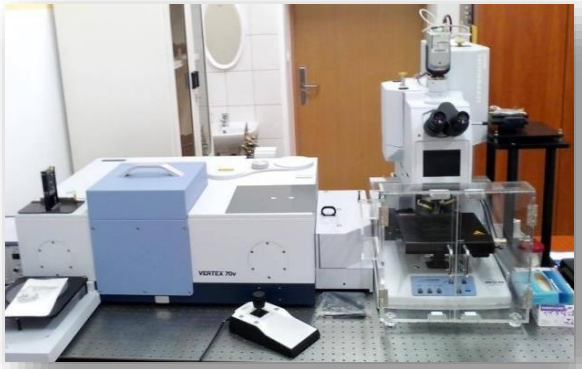

Vacuum FT-IR VERTEX 70V spectrometer with HYPERION 3000 IR microscope

- spectral res.: 4 cm^{-1}
- c ~10^{-4} M

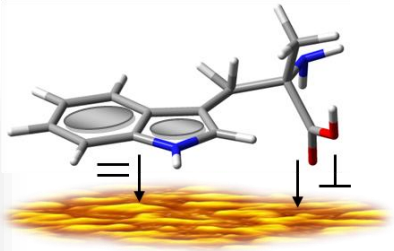

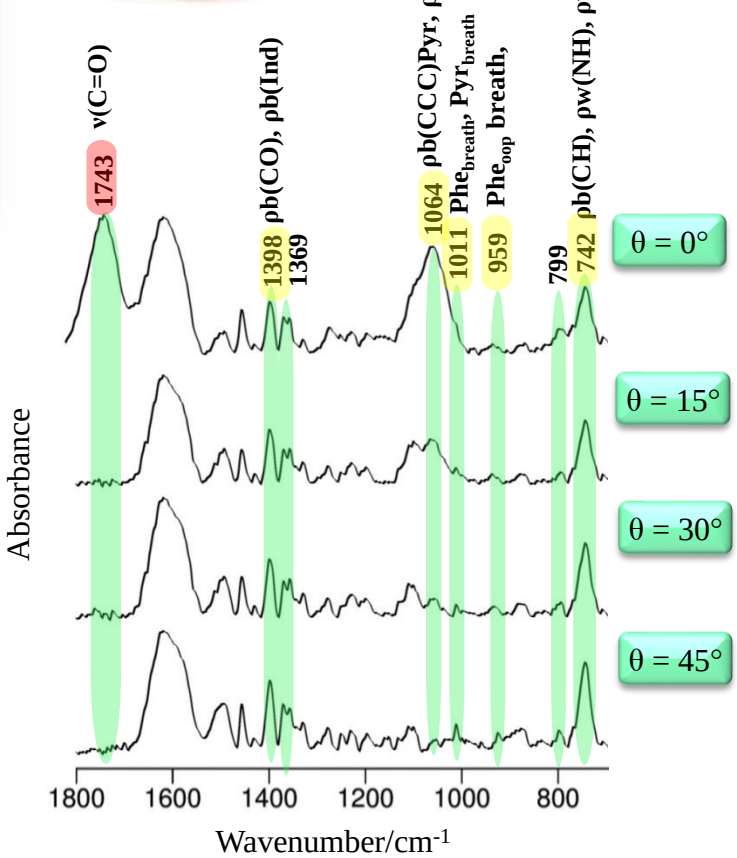

- the spectra were recorded at different incident angles (θ) without changing the sample position
- the angle of incidence changed without shifting the system and focal point of the incident beam, always reflected from the same part of the test sample
- Ind moiety adopts an almost horizontal position on the GNPs
- C=O bond is located perpendicular to the surface, exposing the interaction between the free electron pairs on the oxygen atom and the metal nanostructure

Nocodazole molecular structure

Applied Surface Science 499 (2020) 143975

Contents lists available at ScienceDirect

Applied Surface Science

journal homepage: www.elsevier.com/locate/apsusc

Full Length Article

Physico-chemical analysis of molecular binding to the colloidal metal nanostructure: Multiple micro- and nanospectroscopy study

Ewa Pięta[a,*], Cyril Petibois[b,c], Czesława Paluszkiewicz[a], Wojciech M. Kwiatek[a]

[a] Institute of Nuclear Physics Polish Academy of Sciences, PL-31342 Krakow, Poland
[b] Academia Sinica, Institute of Physics, 128 Sec. 2, Academia Rd., Nankang, Taipei 11529, Taiwan
[c] University of Bordeaux, Inserm U1029 LAMC, Allée Geoffroy Saint-Hillaire, Bat. B2, F33600 Pessac-Cedex, France

nocodazole

(methyl N-[6-(thiophene-2-carbonyl)-1H-benzimidazol-2-yl]carbamate)

- belongs to the class of aromatic heteropolycyclic organic molecules, benzimidazoles
- an antineoplastic agent which exerts its effect in cells by interfering with the polymerization of microtubules
- rapidly depolymerises microtubules in vivo and inhibits tubulin polymerisation in vitro. Inhibits mitosis
- cells treated with this drug arrest in a G2/M phase as a consequence of slower elongation and decreasing velocities of microtubules

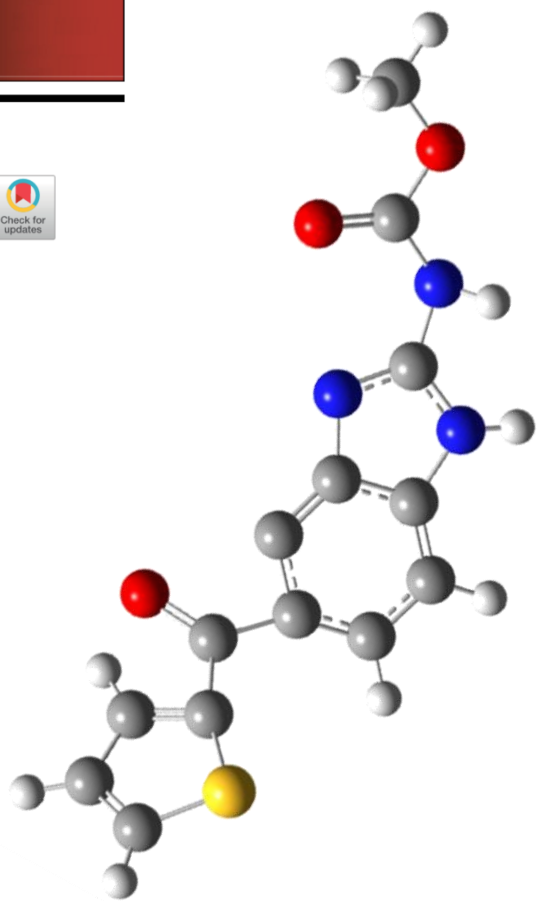

Nocodazole
FTIR & SEIRA studies

Bmd - benzimidazole

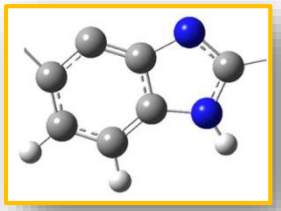

Phe - phenyl

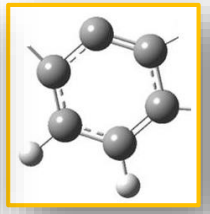

Thp - thiophene

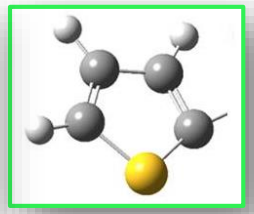

cbt - carbamate

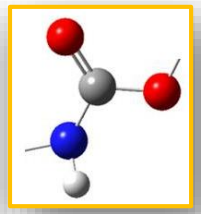

cbn - carbonyl

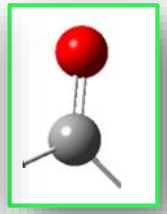

FT-IR VERTEX 70 spectrometer with HYPERION 3000 IR microscope

- transmission mode
- CaF_2 window
- FPA 128x128 detector
- spectral resolution: 4 cm^{-1}
- 256 scans
- c ~10^{-4} M

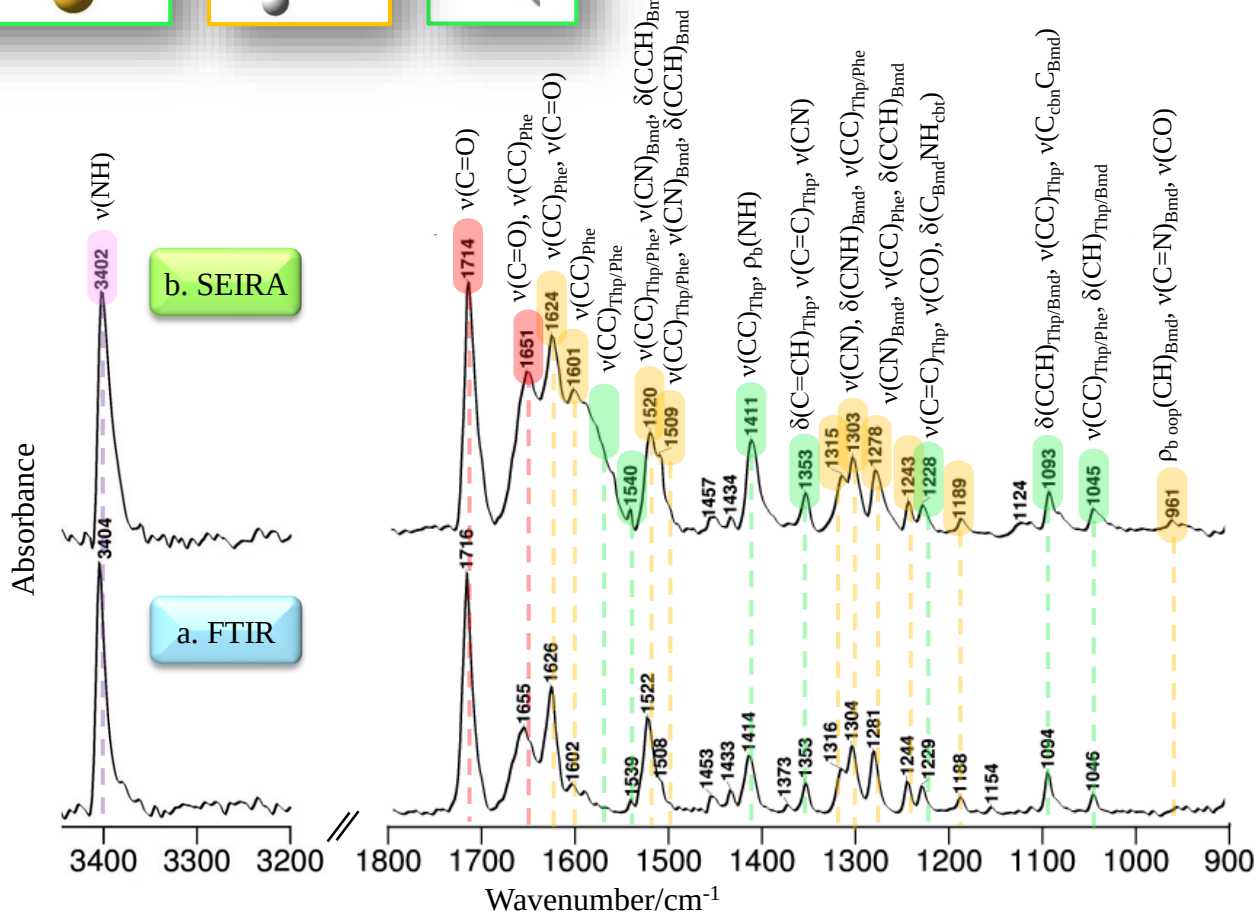

Nocodazole
RS & SERS studies

Bmd - benzimidazole

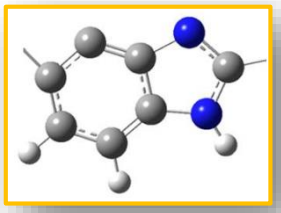

Phe - phenyl

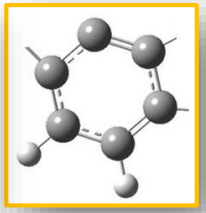

Thp - thiophene

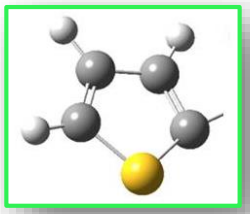

cbt - carbamate

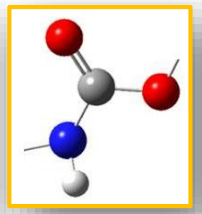

cbn - carbonyl

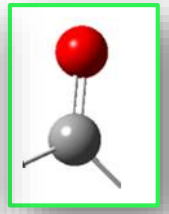

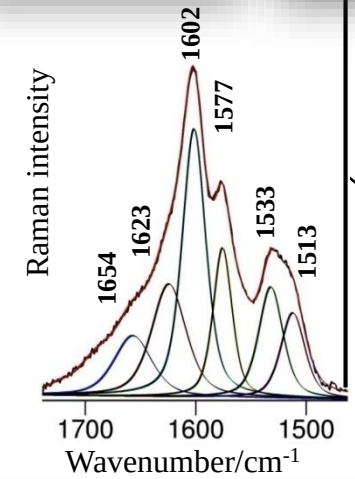

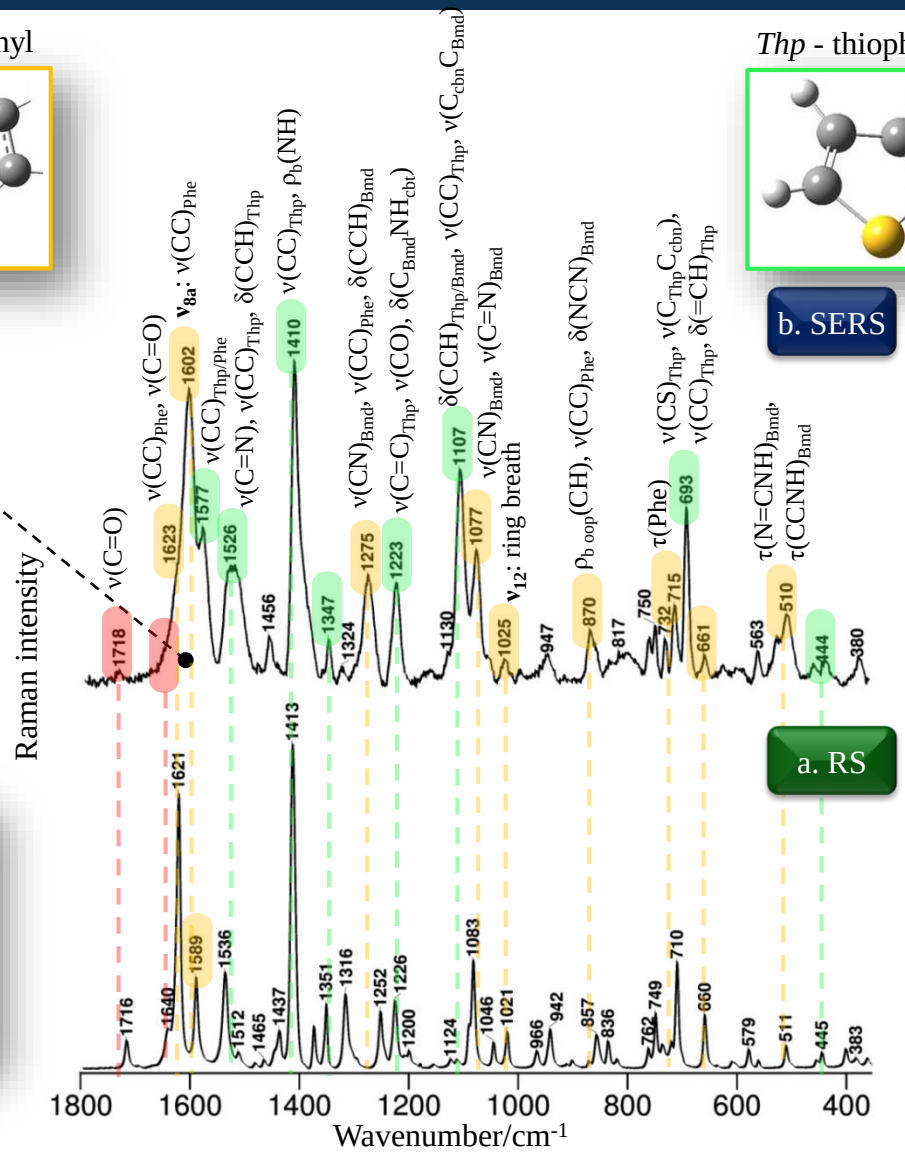

- exc. wavelength: 633 nm
- CCD detector
- 20× magn. objective
- spectral resolution: 1 cm^{-1}
- laser power 10 mW

- exc. wavelength: 633 nm
- CCD detector
- 100× magn. objective
- spectral resolution: 1 cm^{-1}
- laser power 100 mW

InVia Renishaw Spectrometer integrated with atomic force microscope

Nocodazole
RS & SERS studies

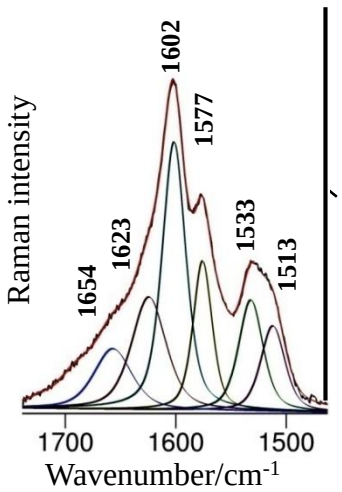

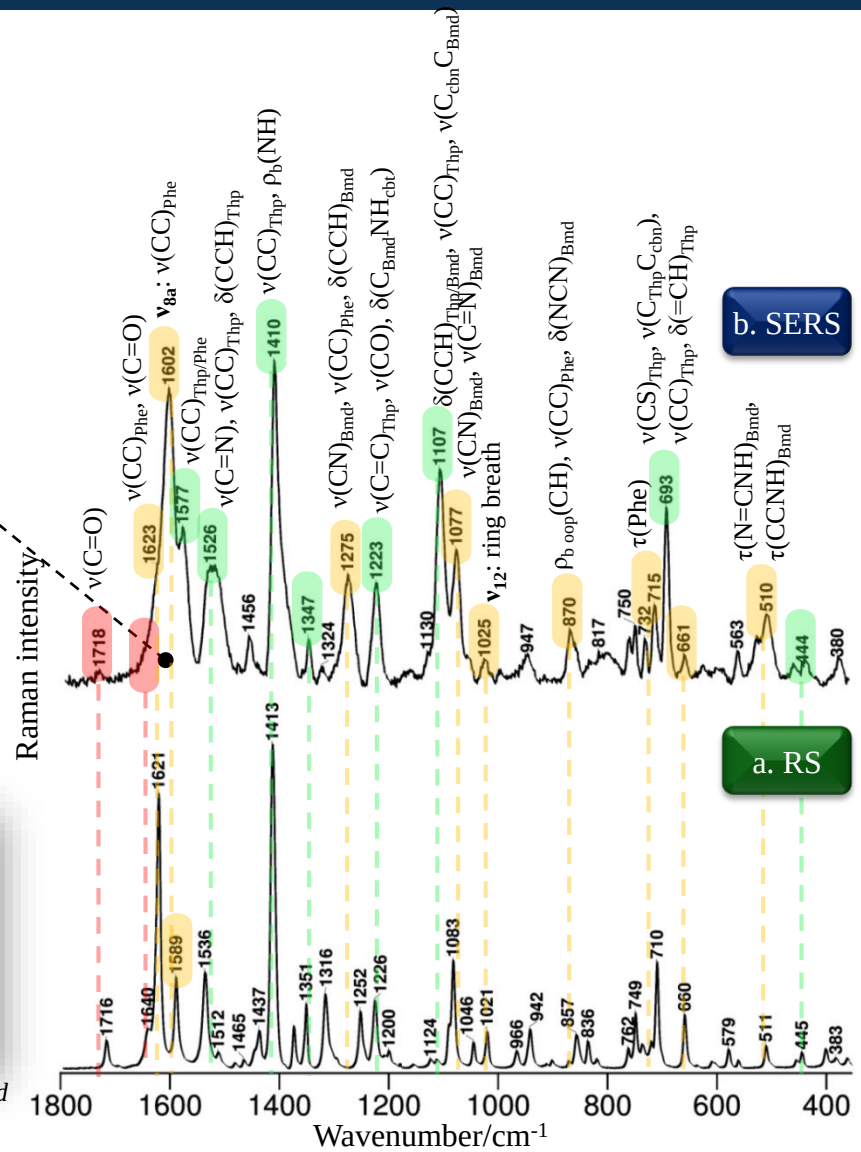

InVia Renishaw Spectrometer integrated with atomic force microscope

- the 1602 cm^{-1} SERS band (ν_{8a} according to the Wilson numbering scheme) shows enormous enhancement and broadening (Δf_{whm} = 16 cm^{-1}) upon adsorption. The band is also significantly blue shifted ($\Delta\bar{\upsilon}$ = 13 cm^{-1}) in comparison to that observed in RS spectrum
- the charge-transfer mechanism contributes significantly to the signal enhancement
- significant decrease in the intensity of the 1025 cm^{-1} band (ν_{12}, ring breathing) in relation to the discussed ν8a spectral signal
- the charge-transfer mechanism can be associated with phenyl and/or imidazole fragments
- *Imd* is an aromatic molecule that possesses six π-electrons, including a pair of electrons on the nitrogen atom placed outside the ring, which may facilitate interaction with the Au-NPs

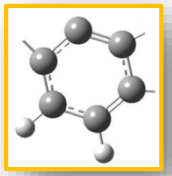

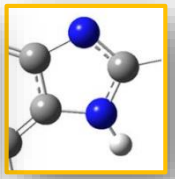

PM–SEIRA nanospectroscopy study

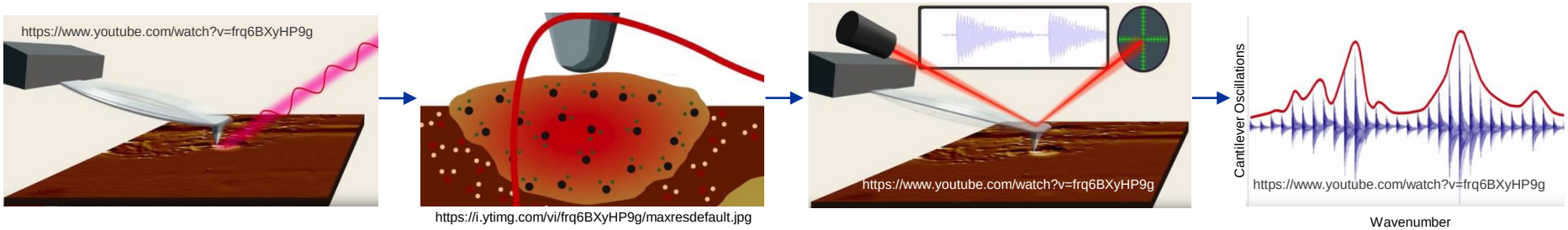

- a sample is illuminated with pulses of infrared radiation
- AFM tip acts as a detector of the absorbed radiation with nanoscale spatial resolution
- IR light absorbed by the sample is converted to heat, causing a rapid thermal expansion pulse under the AFM tip and exciting resonant oscillation of the AMF cantilever
- the amplitude of the cantilever oscillation is directly proportional to the sample absorption coefficient

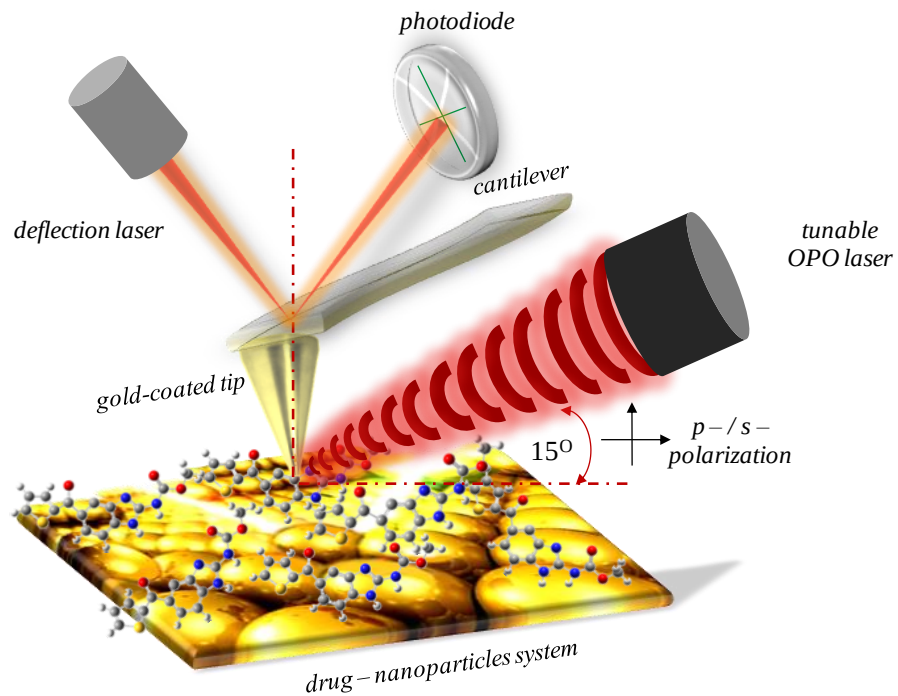

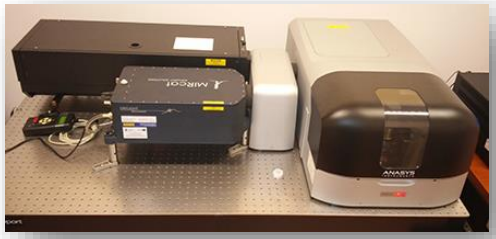

Anasys NanoIR2 AFM-IR system

A. Dazzi, R. Prazeres, F. Glotin, J.M. Ortega, *Opt. Lett.*, 2005, 30, 2388-2390.

Lu, F.; Jin, M.; Belkin, M.A. *Nat. Photonics* 2014, 8, 307-312.

N. Piergies, E. Pięta, C. Paluszkiewicz, H. Domin, W. M. Kwiatek, *Nano Research*, 11, 2018, 4401-4411.

E. Pięta, C. Paluszkiewicz, W. M. Kwiatek, *Phys. Chem. Chem. Phys* 2018, 20, 27992- 28000.

E. Pięta, C. Petibois, C. Paluszkiewicz, W.M. Kwiatek, *Applied Surface Science* 499 (2020) 143975.

PM–SEIRA nanospectroscopy study

- optical parametric oscillator (OPO) laser
- spectral resolution: 4 cm^{-1}
- 256 co-averages
- c ~10^{-4} M
- averaged from 20 spectra

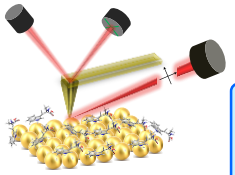

- tracking negligible changes in bonds arrangement
- spectacular changes in relative band intensities
- *p*-polarized incident radiation (parallel to the axis of the tip): the vibrational modes with dipoles located perpendicularly to the gold substrate will be the most pronounced
- *s*-polarization modulation (perpendicular to the axis of the tip): oscillations attributed to the parallel or tilted bonds will be the most enhanced
- strong interaction between the Bmd and the Au-NPs surface
- C–N bond is situated almost parallel to the metal surface → horizontal orientation of Bmd bicyclic group

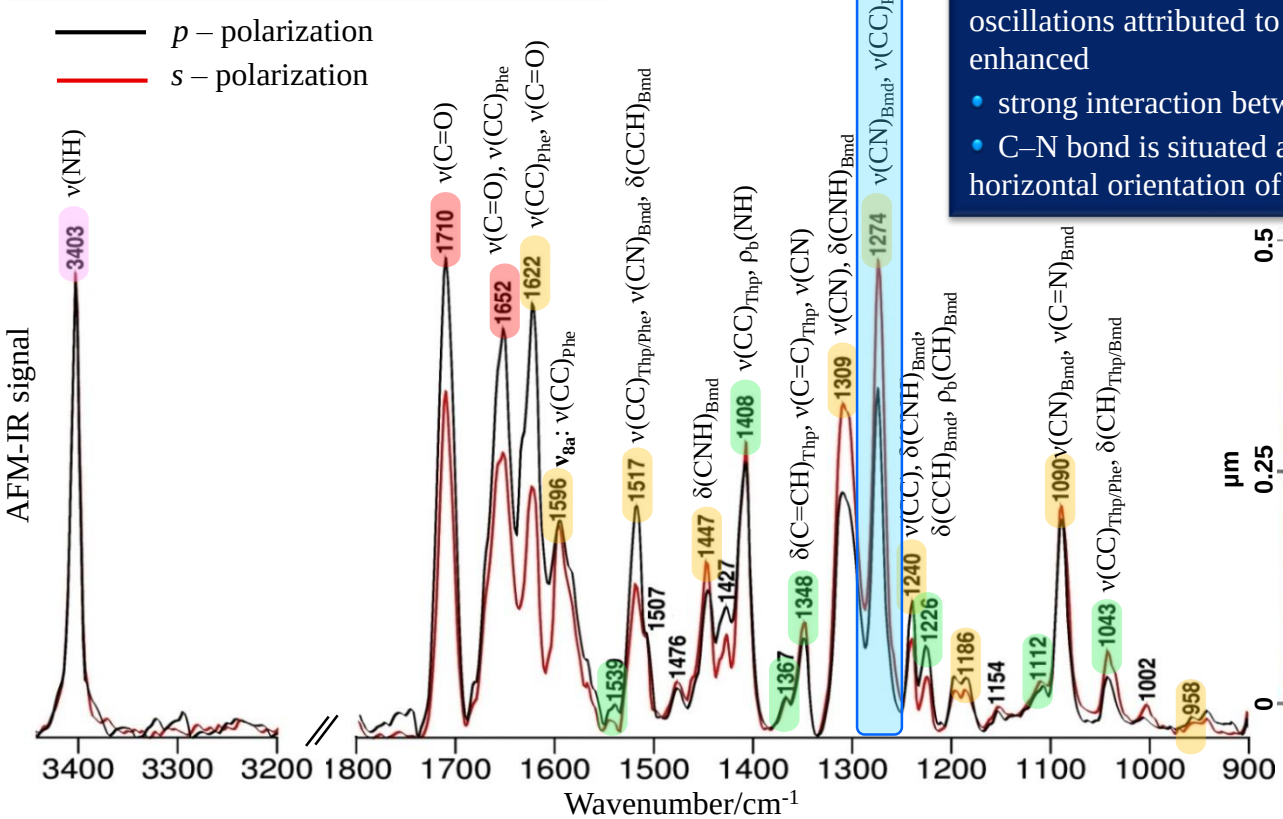

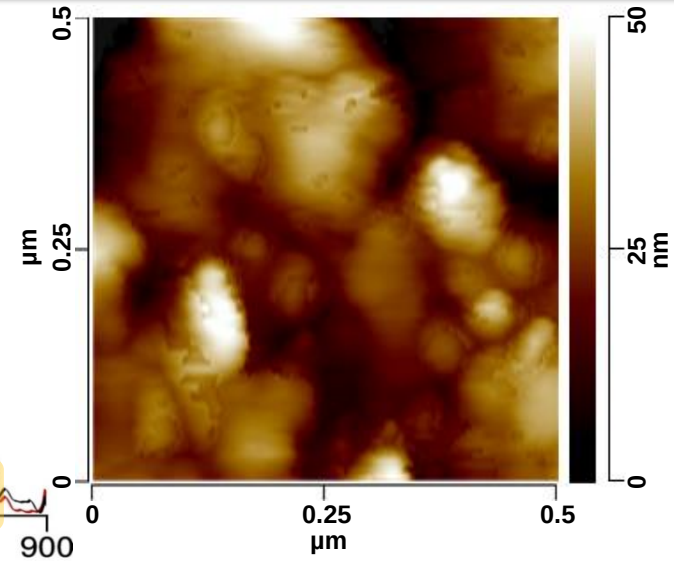

AFM image of the drug – Au-NPs conjugate

E. Pięta, C. Petibois, C. Paluszkiewicz, W.M. Kwiatek, *Applied Surface Science* 499 (2020) 143975.
M. Handke, M. Milosevic and N. J. Harrick, Vib. Spectrosc., 1991, 1, 251–262.
H. A. R. Ras, R. A. Schoonheydt and C. T. Johnston, J. Phys. Chem. A, 2007, 111, 8787–8791.
B. L. Frey, R. M. Corn and S. C. Weibel, Polarization-Modulation Approaches to Reflection Absorption Spectroscopy, in Handbook of Vibrational Spectroscopy, ed. P. R. Griffiths, John Wiley&Sons, New York, 2001, pp. 1042–1056

Deducing the adsorption geometry

Bmd ring is arranged in a direction substantially parallel to the metal surface, favoring the interaction between the free electron pairs and NPs

Thp and Bmd rings dictate the adsorption behavior of nocodazole on the metal nanostructure

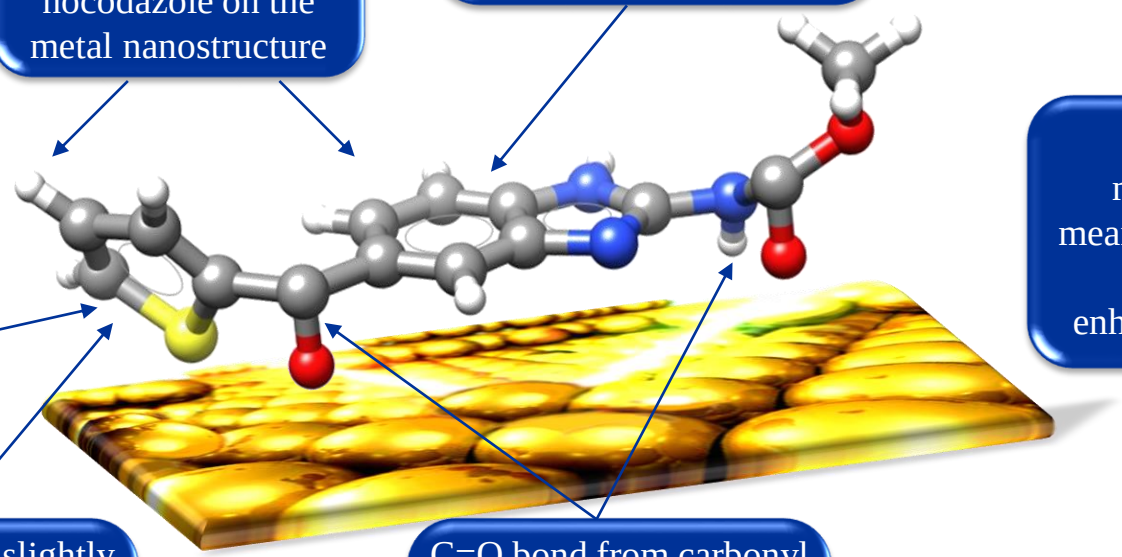

charge-transfer mechanism has a meaningful contribution to the chemical enhancement in SERS

strong interaction between the electron donating, sulfur-containing Thp moiety and the metal substrate

Thp ring with slightly tilted position exposes the interplay between the sulfur atom (the lone electron pairs) and Au-NPs

C=O bond from carbonyl and/or carbamate groups plays a significant role in the adsorption by adopting a vertical orientation

NPs penetration through the cell membrane correlative imaging

- determination of the individual cellular components
- assessment the NPs penetration through the cell membrane
- correlative imaging accessory for single cell correlative imaging
- imaging exactly the same cell using several methods
- nanoparticles accumulate around the nucleus

CORRESCOPY
CORRELATIVE IMAGING

- exemplary 3D Raman map for individual cell
- red color corresponds to the largest accumulation of nanoparticles
- nanoparticles accumulate mainly around the nucleus.

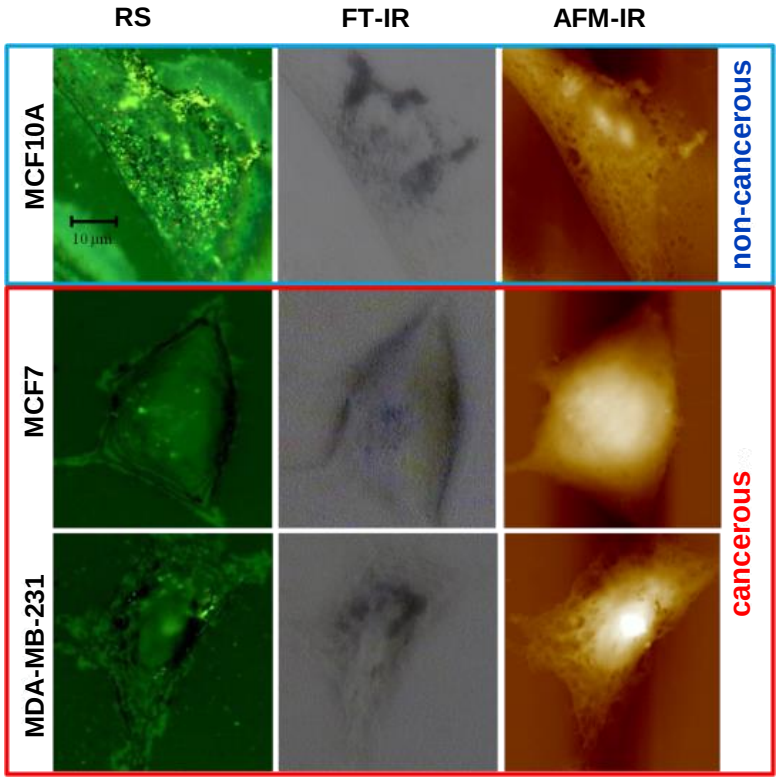

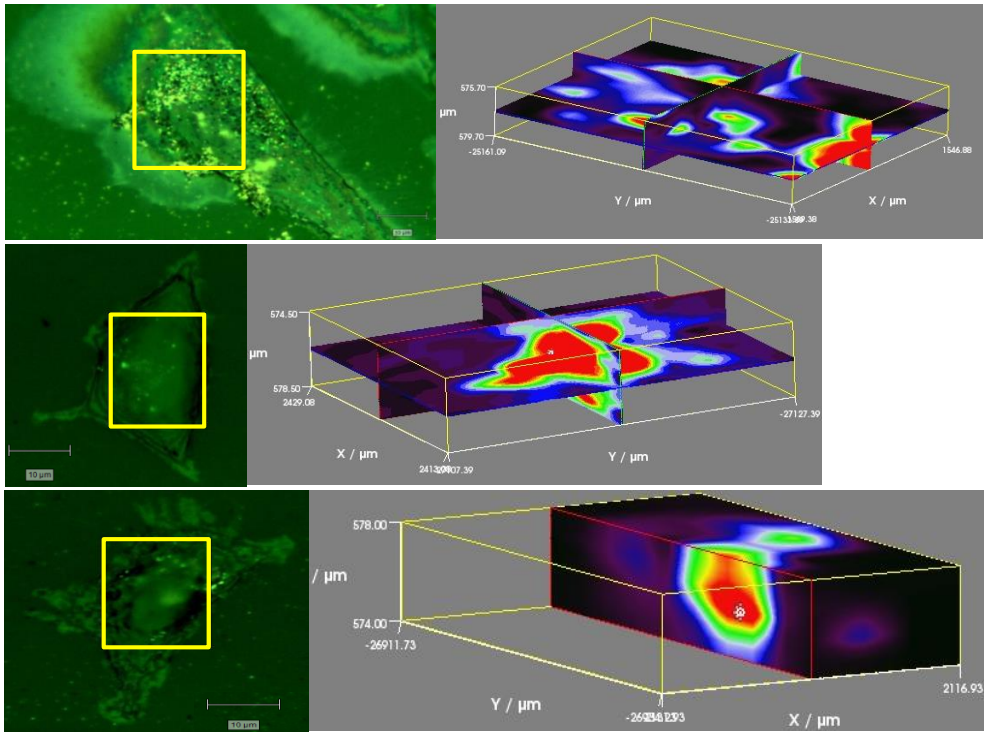

E. Pięta, et. al., *in preparation*

Sensors & Actuators: B. Chemical 313 (2020) 128039

Contents lists available at ScienceDirect

Sensors and Actuators B: Chemical

journal homepage: www.elsevier.com/locate/snb

Assessment of cellular response to drug/nanoparticles conjugates treatment through FTIR imaging and PLS regression study

Ewa Pięta[a,*], Cyril Petibois[b,c], Katarzyna Pogoda[a], Klaudia Suchy[a], Danuta Liberda[a,1], Tomasz P. Wróbel[a,1], Czesława Paluszkiewicz[a], Wojciech M. Kwiatek[a]

[a] Institute of Nuclear Physics Polish Academy of Sciences, PL-31342, Krakow, Poland
[b] Academia Sinica, Institute of Physics, 128 Sec. 2, Academia Rd., Nankang, Taipei 11529, Taiwan
[c] University of Bordeaux, Inserm U1029 LAMC, Allée Geoffroy Saint-Hillaire, Bat. B2, F33600 Pessac-Cedex, France

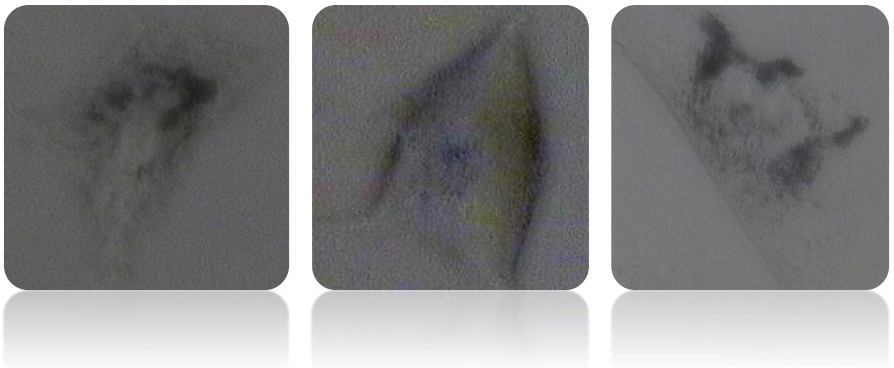

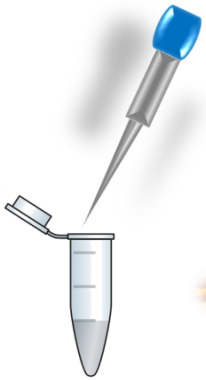

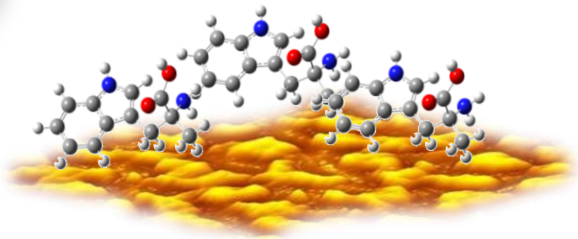

Cell response for drug/NPs conjugates treatment FT-IR imaging

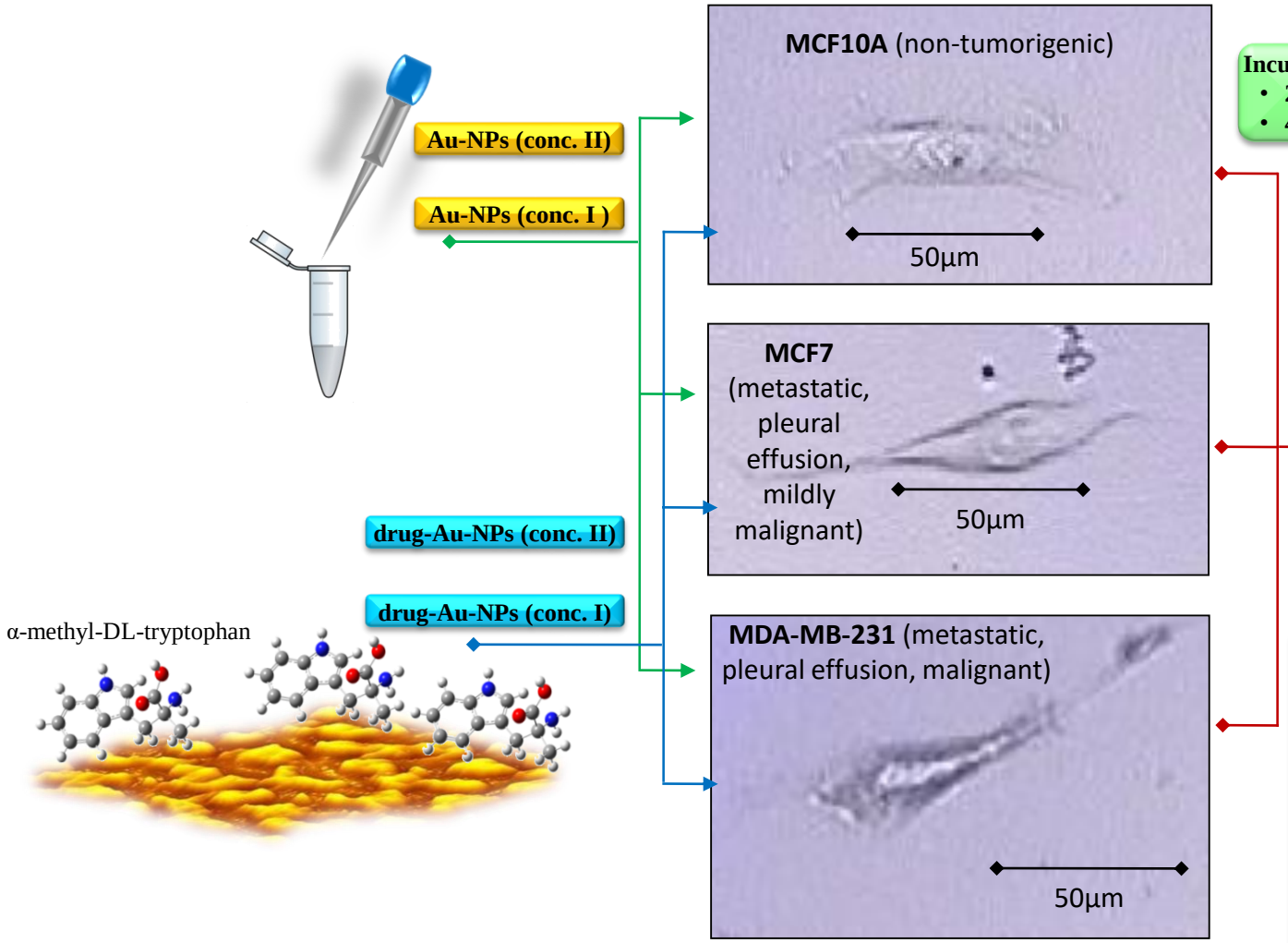

Incubation time:
- **24h**
- **48h**

FT-IR imaging

FT-IR VERTEX 70 spectrometer with HYPERION 3000 IR microscope

- transmission mode
- CaF_2 window
- FPA 128x128 detector
- FTIR maps collected for 10 single cells per each condition, and spectra from each individual cell were averaged (~80 spectra per cell)

Cell response for drug/NPs conjugates treatment MTS viability assay

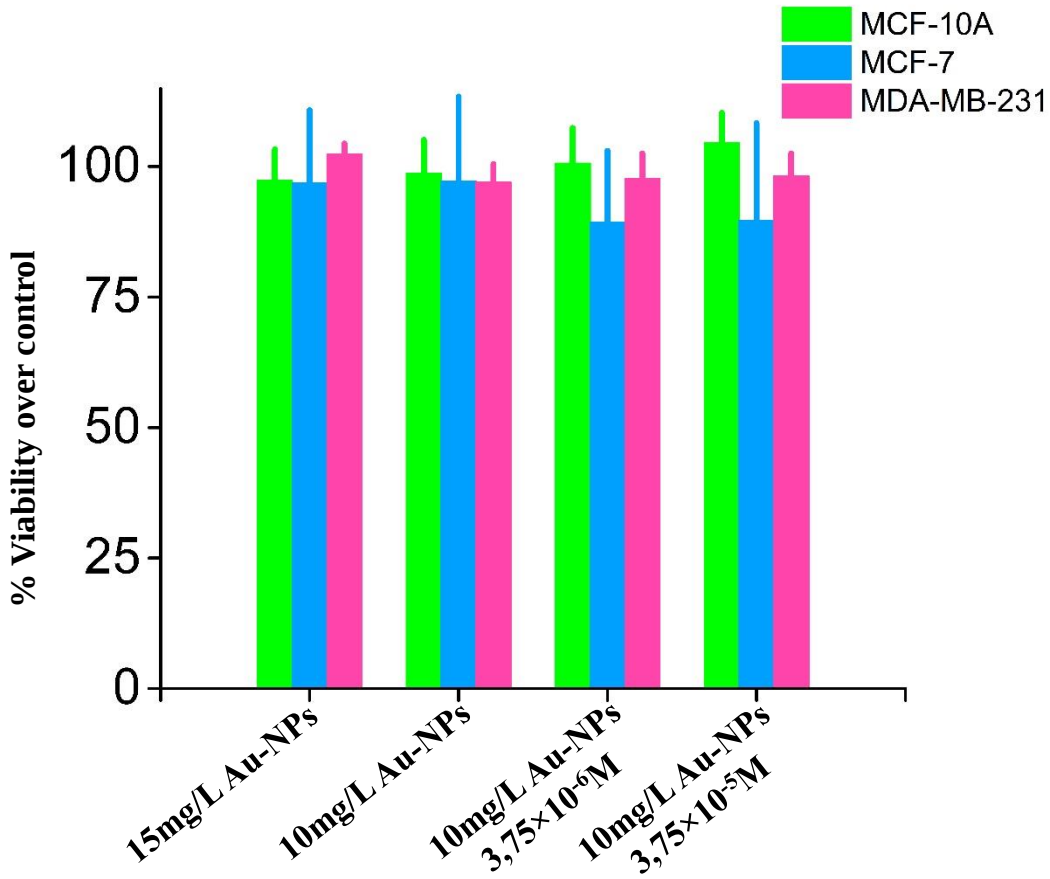

Viability of the MCF-10A, MCF-7 and MDA-MB-231 cells treated with NPs (15mg/L and 10mg/L) and NPs/drug conjugates (10mg/L NPs @ 3,75×10-6M and 10mg/L NPs @ 3,75×10-5M) 48 hours post treatment. The significance of differences was determined with the two-tailed Student's t test using GraphPad online calculator. None of the tested values showed $p < 0.05$ that could be considered to be statistically significant difference.

Cell response for drug/NPs conjugates treatment the average FT-IR spectra

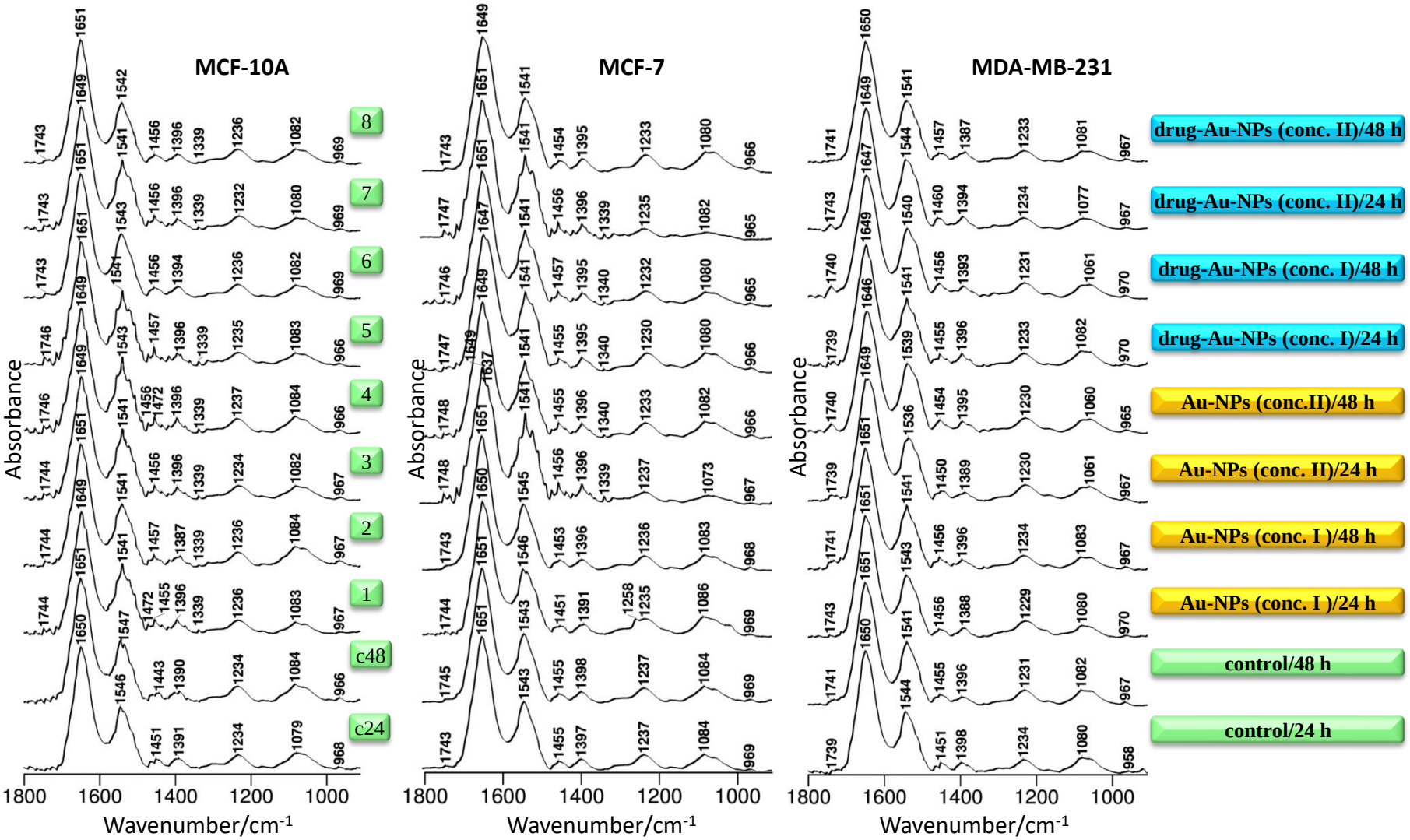

Cell response for drug/NPs conjugates treatment FTIR-PLS regression results

control cells *vs* cells treated with drug/Au-NPs conjugate

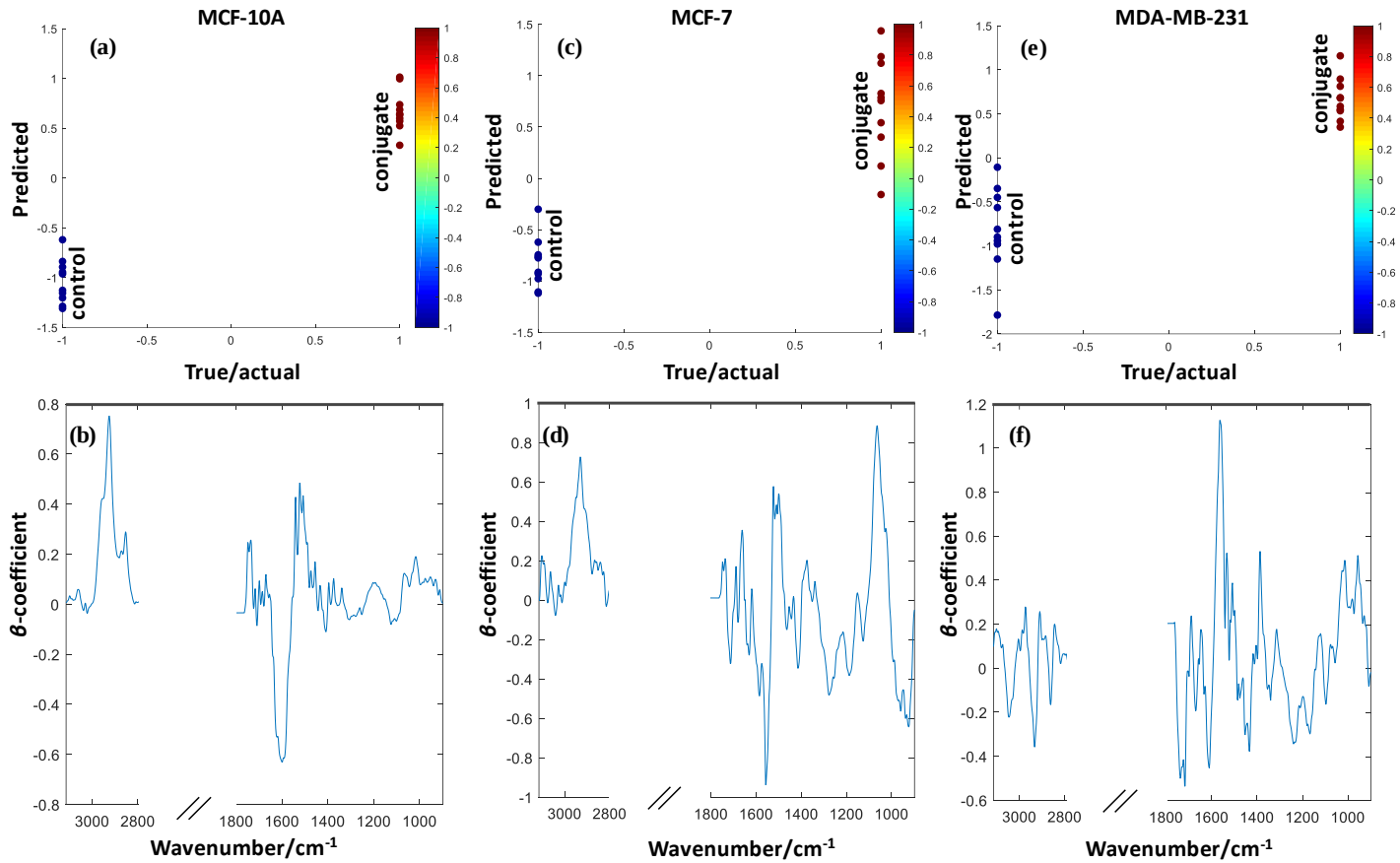

Figure: The partial least squares (PLS) regression results for the studied MCF-10A, MCF-7 and MDA-MB-231 breast cells: control cells and cells after treatment with *α*-methyl-DL-tryptophan ($3{,}75 \cdot 10^{-5}$ M)/AuNPs (10 mg/l) conjugate. Cells were incubated for 48 h. The actual class membership (x-axis) *vs* predicted class values (y-axis) for the control and treated individual cell lines (a, c and e, respectively) along with corresponding *β*-regression coefficients (b, d and f, respectively). The number of LV for MCF-10A, MCF-7 and MDA-MB-231 cell lines was 2, 3 and 3, respectively.

Cell response for drug/NPs conjugates treatment FTIR-PLS regression results

control cells *vs* cells treated with drug/Au-NPs conjugate

MCF-10A

- CH_2/CH_3 vibrations in lipids, amide I and vibrations ν(C=O) from phospholipid esters determine the separation between control and treated cells
- bands due to RNA/DNA have only a negligible contribution to this model

MCF-7

- bands due to RNA/DNA play a predominant role in the separation between cells
- amide I/II, $\nu_{as/s}(CH_2/CH_3)$ in lipids, ν(C=O) in phospholipids, and ν_{as}(CO-O-C) vibrations in cholesterol esters also contribute significantly to the model

MDA-MB-231

- bands due to amide II oscillations are mainly responsible for separation between cells
- bands due to RNA/DNA, CH_2/CH_3 vibrations in lipids and C=O in triglicerides have significant contribution to this model

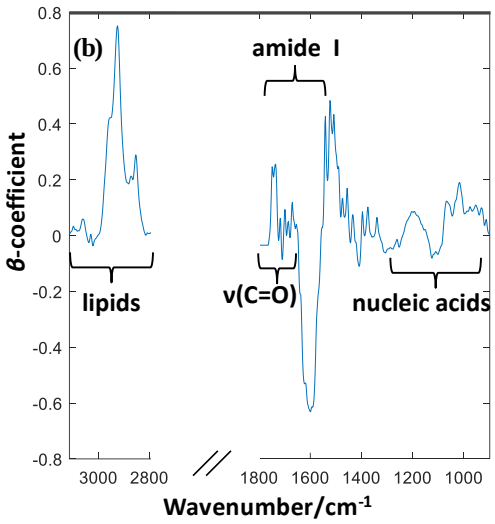

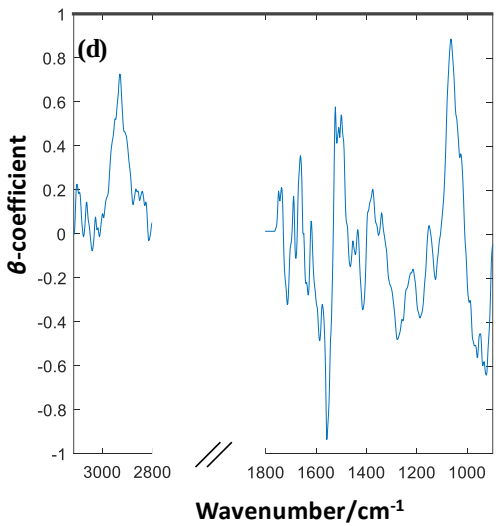

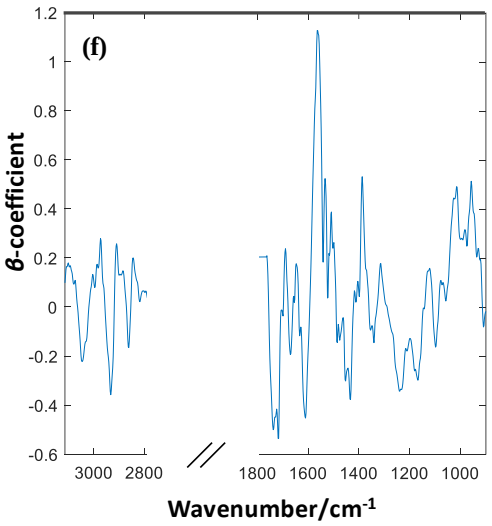

- **Drug/NPs conjugate affects the nucleic acids in all of the studied cell types.**
- **However, the most significant effect was observed in the case of MCF-7 cell line!**

Cell response for drug/NPs conjugates treatment FTIR-PLS regression results

cells treated with Au-NPs *vs* cells treated with drug/Au-NPs conjugate

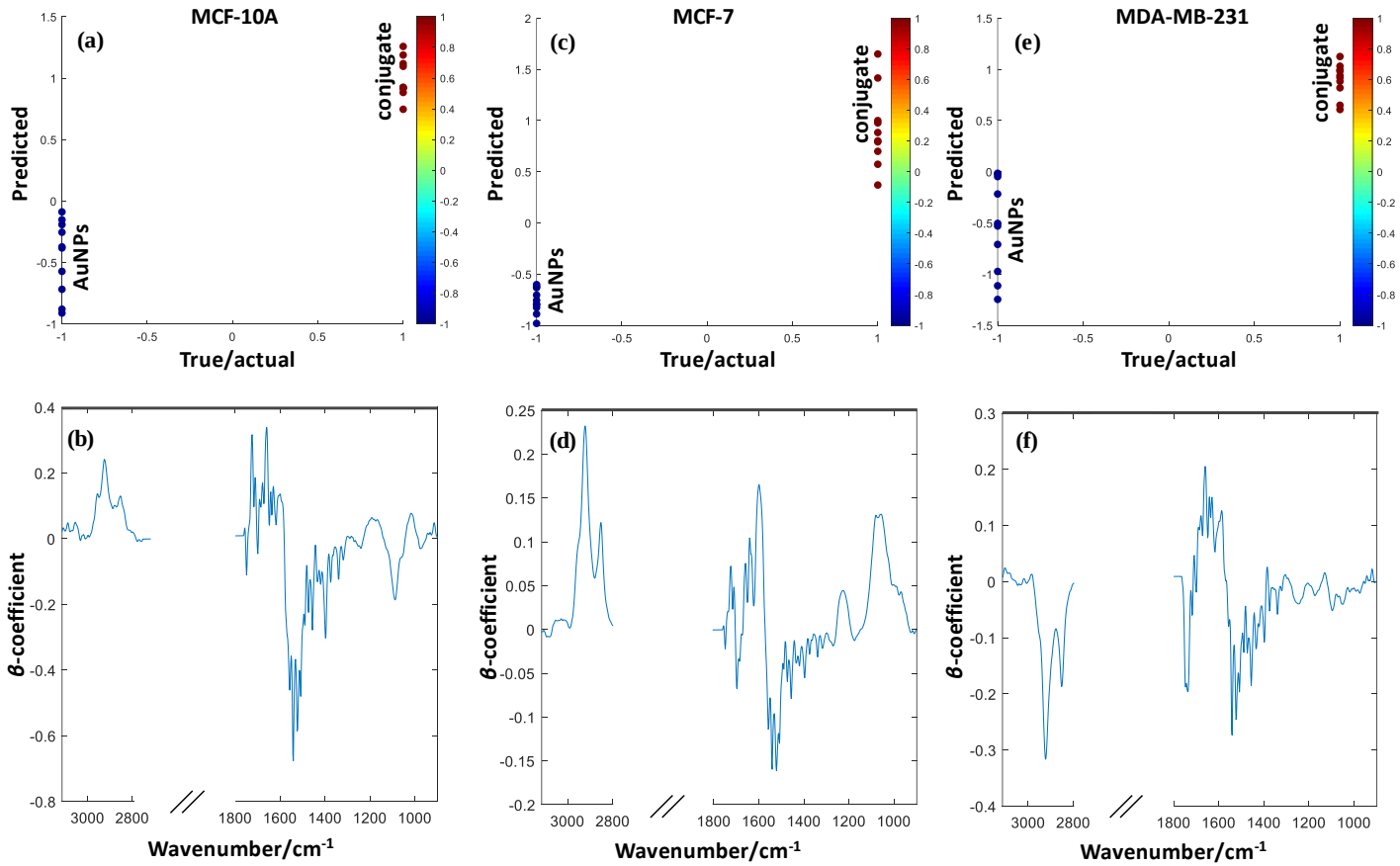

Figure: The partial least squares (PLS) regression results for the studied MCF-10A, MCF-7 and MDA-MB-231 breast cells: cells treated with Au-NPs (10 mg/l) and cells after treatment with α-methyl-DL-tryptophan (3.75 × 10−5 M) AuNPs (10 mg/L) conjugate. Cells were incubated for 48 h. The actual class membership (x-axis) vs predicted class values (y-axis) for the cells treated only with AuNPs and cells treated with drug/AuNPs conjugate (a, c and e, respectively) along with corresponding β-regression coefficients (b, d and f, respectively). The number of LV for MCF-10A, MCF-7 and MDA-MB-231 cell lines was 1, 1 and 2, respectively.

Cell response for drug/NPs conjugates treatment FTIR-PLS regression results

cells treated with Au-NPs *vs* cells treated with drug/Au-NPs conjugate

MCF-10A

Very good separation between the cells can be achieved based on the peaks ascribed to:

- amide I and II (especially the band at ~1544 cm^{-1} (amide II: ρ_b(NH), ν(CN), α-helix) and ~1650 cm^{-1} (amide I: ν(C=O), α-helix)
- lipids ($\nu_{as/s}(CH_3/CH_2)$) and phospholipids (ν(C=O))
- nucleic acids (~1083 cm^{-1} ($\nu_s(PO_2)$) and 1025 cm^{-1} (ν(C–O): deoxyribose))

MCF-7

- spectral features due to nucleic acids oscillation play a predominant role in the separation: 1237 ($\nu_{as}(PO_2^-)$), 1084 ($\nu_s(PO_2^-)$), 1056 ($\nu_s(PO_2^-)$, ν(CC) and ν(CO)), 1025 (ν(C–O)), 965 cm^{-1} (ν(C-N±-C))
- this cell line seems to be particularly sensitive to the drug treatment, which result in drug interacting with nucleic acids and DNA conformational changes
- lipids also make an important contribution to the model

MDA-MB-231

- bands associated with changes in lipids and amide I and II vibrations exhibit the most significant variations between cells
- peaks resulting from nucleic acid vibrations are almost invisible

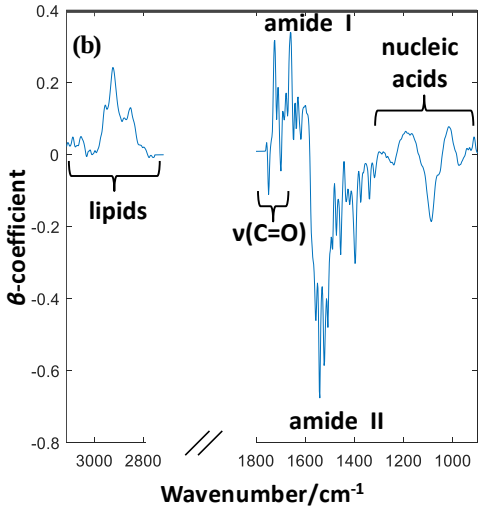

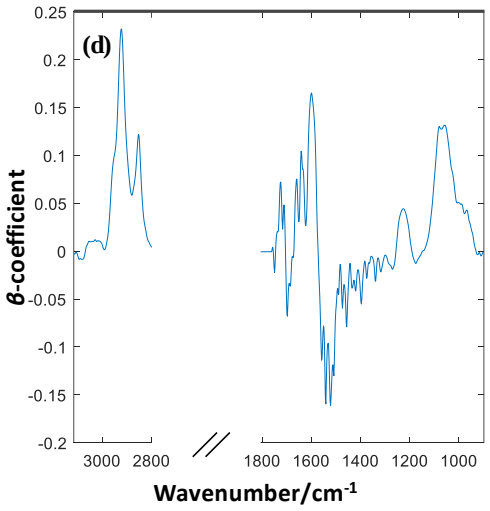

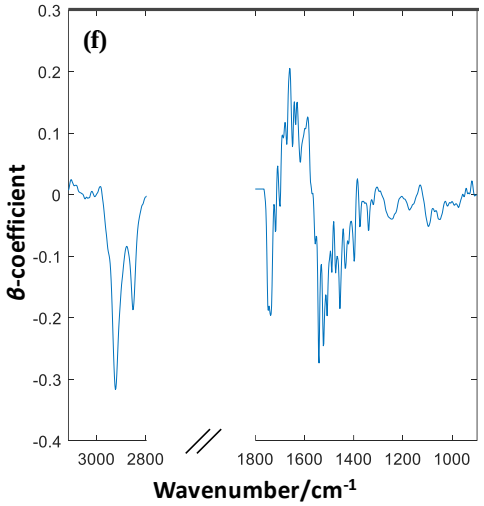

Cell response for drug/NPs conjugates treatment FTIR-PLS regression results

- more prominent changes induced by the AuNPs or drug/AuNPs conjugate occur in the cells cultured for 48 h than 24 h for higher drug concentration
- weak separation between the control cells and cells treated only with AuNPs
- AuNPs can be effectively used in combination with drugs to study sensitivity of cancer cells to drugs, biosensing or bioimaging applications
- longer incubation times

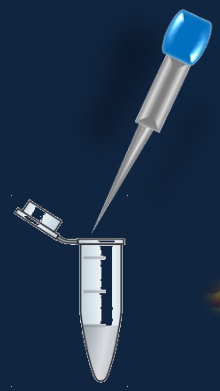

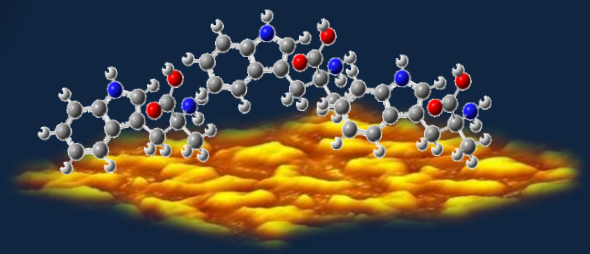

Summary

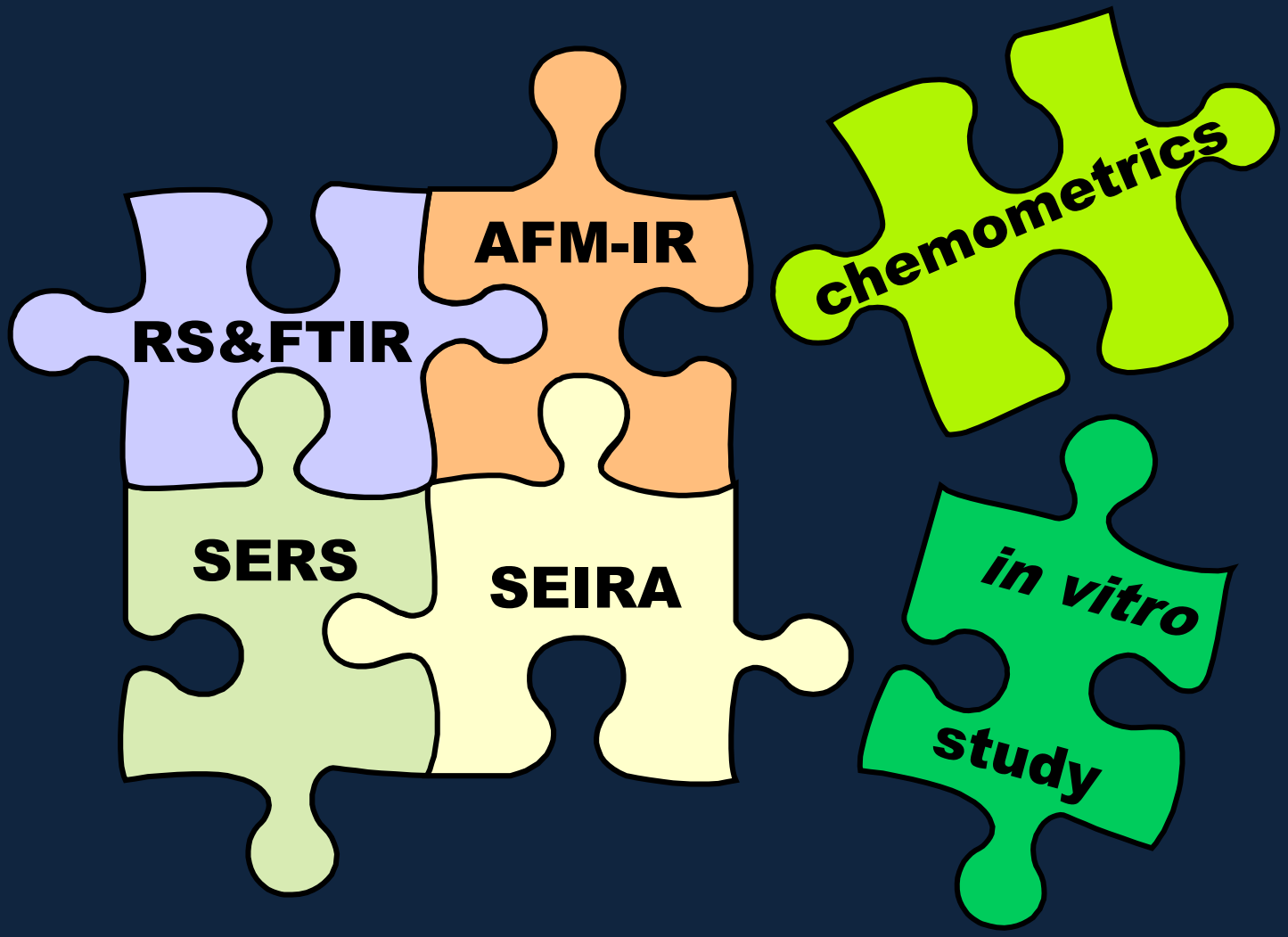

Acknowledgements

dr hab. Czesława Paluszkiewicz, prof. IFJ PAN

prof. dr hab. Wojciech M. Kwiatek

dr Katarzyna Pogoda

dr Natalia Piergies

mgr Klaudia Suchy

Jolanta Adamczyk

Institute of Nuclear Physics
Polish Academy of Sciences

Professor Cyril Petibois

Academia Sinica, Institute of Physics, Taiwan

University of Bordeaux, Pessac-Cedex, France

dr hab. Magdalena Oćwieja

Institute of Catalysis and Surface Chemistry
Polish Academy of Sciences

dr Tomasz Wróbel

mgr Danuta Liberda

SOLARIS
National Synchrotron Radiation Centre

The French Government and the French Embassy in Poland – research stay

National Science Centre, 2017/01/X/ST4/00428

the Małopolska Regional Operational Program Measure 5.1 Krakow Metropolitan Area as an important hub of the European Research Area for 2007–2013, project No. MRPO.05.01.00–12–013/15

Thank you for your kind attention!

Photo courtesy of le.ac.uk.